Polymeric Photorefractive Materials

W. E. Moerner* and Scott M. Silence

IBM Research Division, Almaden Research Center, San Jose, California 95120-6099

Received June 15, 1993 (Revised Manuscript Received September 13, 1993)

Contents

W. E. Moerner was born in 1953 in Pleasanton, CA. After receiving three Bachelor's degrees from Washington University, St. Louis, in 1975, he obtained M.S. (1978) and Ph.D. (1981) degrees in physics from Cornell University, where he worked with Prof. A. J. Sievers. He joined the IBM Research Division, Almaden Research Center in 1981, receiving Outstanding Technical Achievement Awards in 1988 and 1992. He received the Roger I. Wilkinson Outstanding Young Electrical Engineer Award in the U.S. in 1984. He is a Fellow of the American Physical Society, a Fellow of the Optical Society of America, a Senior Member of the Institute of Electrical and Electronics Engineers, and a member the American Chemical Society. His current interests involve polymeric photorefractive materials, single-molecule spectroscopy in solids, and novel optical storage mechanisms.

Scott M. Silence was born in 1964 in Passaic, NJ. He studied chemistry at the University of Chicago, where he obtained B.S. and M.S. degrees in 1986, and physical chemistry at the Massachusetts Institute of Technology under the direction of Prof. Keith Nelson, where he received a Ph.D. in 1991. In 1991 he joined the staff of the IBM Almaden Research Center as a visiting scientist. His research interests center on nonlinear optics and materials, including using nonlinear optical processes to study structural changes in condensed media and study of the photorefractive effect in organic polymers.

I. Introduction

The photorefractive (PR) effect is defined as spatial modulation of the index of refraction due to charge redistribution in an optically nonlinear material. The effect arises when charge carriers, photogenerated by a spatially modulated light intensity, separate by drift and diffusion processes and become trapped to produce a nonuniform space-charge distribution. The resulting internal space-charge electric field then modulates the refractive index to create a phase grating which can diffract a light beam. This definition of photorefrac-

0009-2665/94/0794-0127$14.00/0

Table 1. Figure of Merit, Q, for Inorganic[a] and Organic Materials

material	electrooptic coefficient: r (pm/V)	refractive index: n	dielectric constant: ϵ_r	Q (pm/V)
$Bi_{12}SiO_{20}$	5	2.54	56	1.5
GaAs	1.43	3.4	12	4.7
$BaTiO_3$	1640	2.4	3600	6.3
$LiNbO_3$	31	2.2	32	10.3
$KNbO_3$	380	2.3	240	19.3
$(Sr,Ba)Nb_2O_6$	216	2.3	750	3.5
organic crystal (potential)	67	2.0	3.2	168
organic polymer (potential)	30	1.6	4.0	31
photorefractive polymer (to date)[b]	3.1	1.7	7.0	2.2

[a] From ref 5. [b] From ref 20.

tivity, which is clearly more specific than the literal interpretation "optical modulation of the index of refraction", has been in use for more than 25 years in the inorganic crystal community, where the effect was first observed in $LiNbO_3$ in 1967.[1] In fact, until very recently, all materials showing the PR effect have been inorganic crystals and they have been the subject of numerous reviews and monographs.[2-9] Other examples of inorganic crystals in which the PR effect has been examined theoretically and experimentally are $LiNbO_3$, $BaTiO_3$, $Bi_{12}SiO_{20}$ (BSO), $Sr_xBa_{1-x}NbO_3$, InP:Fe, GaAs, multiple-quantum-well materials, and several others.[5] Throughout the history of the PR effect in inorganic crystals, a variety of potentially important applications have been proposed,[2-9] including high-density optical data storage, many image processing techniques, phase conjugation, beam fanning limiters, simulations of neural networks and associative memories, and programmable optical interconnection. However, the difficult crystal growth and sample preparation required for inorganics has limited the widespread use of these applications.

Many other mechanisms exist which can modify the index of refraction of a material in response to an optical beam, such as photochromism, thermochromism, thermorefraction, generation of excited states, conventional electronic $\chi^{(3)}$, and so forth.[10,11] All of these local mechanisms, however, lack the nonlocal property of the PR effect arising from the physical motion of charges in the material, usually over a distance on the order of micrometers. This charge transport gives rise to a spatial phase shift between the incident light intensity pattern and the refractive index modulation. An important consequence of this phase shift is energy transfer between two light beams interfering in a PR medium, called asymmetric two-beam coupling (2BC). If the coupling is sufficiently strong, the 2BC gain may exceed the absorption and reflection losses of the sample, and optical amplification can occur. This cannot occur with any local mechanism of index change (unless the material or the light intensity pattern is translated at a particular rate[12]). Many of the most novel applications[2-9] that have been proposed rely on net 2BC gain, including coherent image amplification, novelty filtering, self-phase conjugation, beam fanning limiters, and simulations of neural networks and associative memories.

There are several reasons for pursuing the development of organic photorefractive materials and polymeric PR materials, in particular. One motivation comes from a consideration of a particular figure-of-merit that compares the index change possible in different materials (assuming equal densities of trapped charges). This figure-of-merit may be defined as $Q = n^3 r_e/\epsilon_r$, where n is the optical index of refraction, r_e is the effective electrooptic coefficient, and ϵ_r is the dc dielectric constant relative to the permittivity of free space ϵ_0. Thus Q approximately measures the ratio of the optical nonlinearity to the screening of the internal space charge distribution by medium polarization. Table 1 shows a comparison of the measured Q values for inorganics along with estimated possible values for Q in organic crystals and polymers. For inorganics, it is well known that Q does not vary much from material to material, which is a result of the fact that the optical nonlinearity is driven chiefly by the large ionic polarizability. For organic nonlinear materials, the nonlinearity is a molecular property arising from the asymmetry of the electronic charge distributions in the ground and excited states.[13] For this reason, in organics large electrooptic coefficients are not accompanied by large dc dielectric constants, thus a potential improvement in performance of up to a factor of 10 is possible with organic photorefractives as was recognized several years ago.[14]

In 1990, the first observation of the PR effect in an organic material utilized a carefully grown nonlinear organic crystal 2-(cyclooctylamino)-5-nitropyridine (COANP) doped with 7,7,8,8-tetracyanoquinodimethane (TCNQ).[15,16] The growth of high-quality doped organic crystals, however, is a very difficult process because most dopants are expelled during the crystal preparation. Polymeric materials, on the other hand, can be doped with various molecules of quite different sizes with relative ease. Further, polymers may be formed into a variety of thin-film and wave guide configurations as required by the application. The second-order nonlinearity of polymers containing nonlinear chromophores can be produced by poling, whereas in crystals one may only consider the relatively rare subset of crystals with noncentrosymmetric crystal structures.

Photorefractive polymers are now a reality, and this review presents the current status of this field on the basis of work accepted for publication as of June 1993. Throughout this paper, we take the position that to be regarded as a PR polymer, proof must be presented that photorefractivity is the dominant mechanism of holographic grating formation, rather than photochromism, electrochromism, excited-state gratings, or other local effects. Section II reviews the fundamentals of the PR effect by first describing the necessary elements for photorefractivity, the physical properties which distinguish the organics from the more well-known inorganic PR materials, measurement of these properties, and the grating measurements and asym-

metric two-beam coupling studies required to prove that a given material is indeed photorefractive.

Section III provides a summary of each of the reported PR polymer materials. The first proven polymeric photorefractive material[14,17] was composed of the nonlinear epoxy polymer bisphenol A diglycidyl diether 4-nitro-1,2-phenylenediamine (bisA-NPDA)[18] made photoconductive by doping with the hole-transport agent (diethylamino)benzaldehyde diphenylhydrazone (DEH) (for structures see Figures 8 and 9). This material provided a proof-of-principle that the simultaneous requirements of optical nonlinearity, charge generation, transport, trapping, and absence of interfering photochromic effects can be combined in one material to produce photorefractivity. An earlier publication described a polymeric material showing the necessary requirements of photoconductivity and optical nonlinearity,[19] but this material should be regarded as *potentially* photorefractive until proof is presented of photorefractive grating formation.

The bisA-NPDA:DEH material illustrates one method of formulating a potentially photorefractive polymer: doping a nonlinear host polymer with molecules providing charge transport. Other approaches to PR polymers involve doping a photoconductive polymer with nonlinear optical (NLO) chromophores or synthesizing a fully functionalized material with all functional components attached to the backbone. Examples in each of these categories will be presented, with special emphasis on the recently discovered very large PR response and net two-beam coupling gain in a material composed of poly(*N*-vinylcarbazole) (PVK), doped with 3-fluoro-4-(*N*,*N*-diethylamino)-β-nitrostyrene (FDEANST) and sensitized for charge generation with 2,4,7-trinitro-9-fluorenone (TNF).[20]

Although little detailed theoretical work has been completed on PR polymers, section IV presents a summary of three theoretical issues treated so far: the role of mobility and photocharge generation efficiency in limiting the speed of the response, rate-equation models for the production of the internal space–charge field, and a novel orientational enhancement effect operative in some of the newest materials. Section V concludes with a comparison of PR polymers to the inorganic crystals, with future prospects.

II. Fundamentals of Photorefractivity

A. Necessary Elements for Photorefractivity

The PR effect can occur in certain materials which both photoconduct and show a dependence of the optical index of refraction upon electric field. The ingredients necessary for producing a PR-material are therefore: a photoionizable charge generator, a transporting medium, trapping sites, and a dependence of the index of refraction upon space–charge field. However, the simple presence of these elements in a material does not guarantee that any diffraction grating produced by optical illumination arises from the photorefractive effect.

It is instructive to review in Figure 1 the microscopic processes required to produce a hologram by the PR mechanism, drawing from the considerable body of prior work on the inorganics.[6] Figure 1a shows the optical standing wave pattern of intensity that is produced by

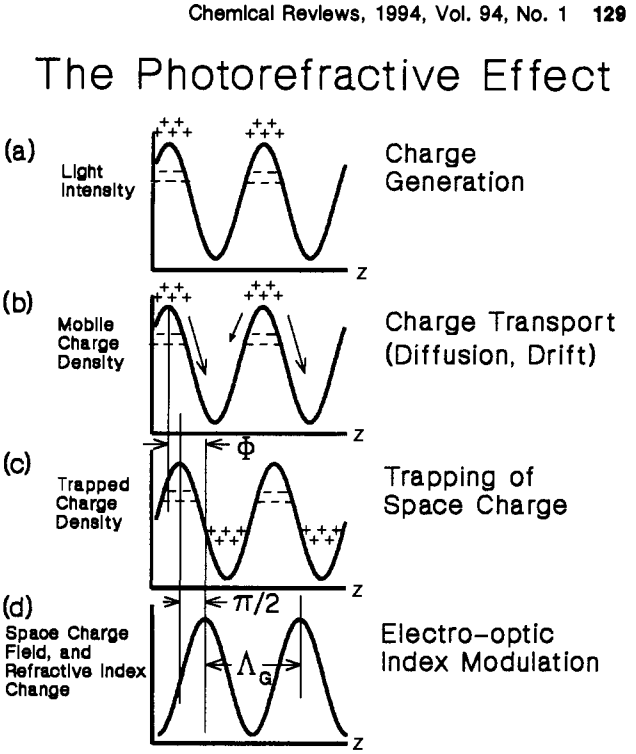

Figure 1. Illustration of photorefractive grating formation, adapted from ref 47: (a) charge generation occurs at the light intensity maxima; (b) the mobile photogenerated charges (holes) then migrate by diffusion or drift in the presence of an external field; (c) the charges trap at the light intensity minima, which (d) creates a space–charge field which leads to a refractive index grating in materials which are electrooptically active. The phase of the space–charge field (and refractive index change) is shifted by Φ from the light intensity pattern. For purely diffusive or purely drift-induced charge motion, $\Phi = \pi/2$.

two intersecting coherent beams of light. This time-independent but spatially modulated intensity pattern consists of light and dark planes throughout the intersection region, which has a spatial wavelength or periodicity Λ_G given by

$$\Lambda_G = \frac{\lambda_0}{2n \sin[(\theta_2 - \theta_1)/2]} \quad (1)$$

where n is the index of refraction of the material, λ_0 is the optical wavelength in free space, and θ_1 and θ_2 are the internal angles of incidence of the two writing beams relative to the sample normal. For easily accessible opening angles between the two light beams and optical wavelengths, the grating wavelength is in the range 0.3–20 μm. The direction normal to the light and dark planes is taken as the direction of the grating wavevector $\vec{K}_G$, the magnitude of which is given by the usual formula $K_G = 2\pi/\Lambda_G$. If one denotes the z axis as the direction of the grating wave vector, the optical intensity follows the offset sinusoidal pattern shown in Figure 1a.

The first physical process required for the PR effect is the generation of mobile charge in response to the spatially varying illumination. This may be viewed as the separation of electrons and holes induced by the absorption of the optical radiation, denoted as plus and minus charges in the figure. In organic materials, this effect is likely to be strongly field dependent (see section II.B).

The second element for the PR effect is transport of the generated charges, with one carrier being more

mobile than the other. In Figure 1b, the holes are shown to be more mobile, which is the more common case for organics. (If both carriers are equally mobile, the resulting space–charge distribution could have zero internal electric field and hence no PR effect.) The physical processes giving rise to charge transport are either diffusion due to density gradients, or drift in an externally applied electric field. Since most polymeric materials with sufficient optical transparency are relatively good insulators, the ability of generated charges to move by diffusion alone is quite limited. In essentially all of the cases described in this review, drift is the dominant mechanism for charge transport which stimulates charge to hop from transport molecule to transport molecule.

The third element for the PR effect, especially when long grating lifetimes are desired, is the presence of trapping sites which hold the mobile charge. In real materials, the exact identity of the trapping sites is seldom known in detail. In general terms, a trapping site is a local region of the material where the mobile charge is prevented from participating in transport for some period of time. For example, in a hopping picture, a site with lower total energy for the charge may act as a trap, and the lifetime of the carrier in the trap will be determined by the trap depth compared to thermal energies.

After separation of charge carriers occurs, the resulting space–charge density is shown in Figure 1c. Via Poisson's equation of electrostatics, such a charge distribution produces a sinusoidal space–charge electric field as shown in Figure 1d. Since Poisson's equation relates the spatial gradient of the electric field to the charge distribution, the resulting internal electric field is shifted in space by 90° relative to the trapped charge, or one-quarter of the grating wavelength.

Finally, if the optical index of refraction of the material changes in response to an electric field, a spatial modulation of the index of refraction results as shown in Figure 1d. For example, if the material has a linear electrooptic effect, the magnitude of the index modulation Δn is related to the magnitude of the space–charge field E_{sc} by the relation

$$\Delta n = -(1/2)n^3 r_e E_{sc} \qquad (2)$$

where r_e is the effective electrooptic coefficient for the geometry under consideration. A sinuosoidally varying index modulation is a grating which can diffract light. If the material is much thicker then an optical wavelength, the grating is actually a volume hologram,[21] and readout of the grating occurs only when the Bragg condition is satisfied.

The total spatial phase shift between the peaks of the optical intensity pattern in Figure 1a and the peaks of the index of refraction modulation in Figure 1d is denoted Φ. In the inorganics where charge diffusion is dominant (with zero external electric field), $\Phi = \pi/2$, which means that a 90° spatial phase shift exists between the light pattern and the index modulation. As an external electric field is applied and drift and diffusion compete, Φ can depart from $\pi/2$, but at sufficiently high fields where the drift mechanism for photoconduction is dominant, Φ again approaches $\pi/2$. Thus in organics where high fields are generally required and diffusion is weak or absent, Φ approaches the $\pi/2$ value, as shown in section III.A.1.a. Such a nonlocal grating cannot occur by any of the nonphotorefractive local mechanisms of grating formation, as charge transport over a macroscopic distance is required.

The PR effect, as defined, is distinct from the many other possible mechanisms of grating formation in optical materials, such as photochromism, thermochromism, thermorefraction, generation of excited states, conventional $\chi^{(3)}$, and so forth.[10] In any report claiming photorefractivity in a new material, the dominance of the PR process over these other interfering processes must be conclusively proven. This is crucial, because many of the most novel applications of photorefractives,[7] such as beam fanning,[22] novelty filtering,[23,24] and self-phase conjugation[25,26] rely upon the presence of a nonzero spatial phase shift between the index of refraction grating and the optical intensity (interference) pattern, or equivalently, asymmetric two-beam coupling (see section II.E). In addition, as long as moving gratings and/or ac electric fields are not used,[6,27] a nonzero phase shift is in fact firm proof that the grating formed is nonlocal and due to charge generation, transport, and trapping in an electrooptic material, i.e., the true photorefractive effect and not a purely local process.[10] Thus, the mere presence of photoconductivity and electrooptic effect are only necessary, but not sufficient, to guarantee that a given material shows detectable photorefractivity. It is worth noting that the charge generation process produces not only a mobile carrier, but also an immobile ion in most cases. The absorption spectrum from the immobile ions can give rise to a photochromic grating which is clearly in phase with the intensity pattern, and this effect has been observed in inorganic crystals.[28] The components of the PR polymer must be carefully designed or the wavelength of operation must be chosen to minimize this effect.

B. Special Properties of Organic Photorefractive Polymers

Several physical effects are operative in organic materials which are not present in the inorganic crystals. First, the quantum efficiency of charge generation ϕ is expected to be highly field dependent. Absorption of a photon creates a bound electron–hole pair (a Frenkel exciton), and separation of this pair to create a free hole competes with geminate recombination, resulting in an electric field dependence for ϕ which may follow the Onsager form.[29] This is widely observed in organic photoconductors[30–33] and is in contrast to the behavior of inorganic photorefractives, where ϕ is independent of field.

Second, in inorganic photorefractive crystals, the mobility is reasonably independent of the electric field. In molecularly doped organic polymers however, the mobility of the photogenerated charges is field dependent (and temperature dependent), with the mobility increasing as $\log (E)^{1/2}$ in many cases as described in several recent reviews.[34–38] This behavior has been verified in several PR polymers.[39–41] The mobility is also strongly dependent upon the interparticle separation between the transport molecules,[35] which means that the transport molecules must be present in high concentration in order to form a connected network for

the hopping of carriers. In many cases, addition of polar dopant molecules or the use of polar host polymers has been shown to reduce the observed mobility.[42] (Doped poly(silane) materials provide a counterexample to this trend,[42,43] see section IV.A.) Since the NLO chromophores required for the PR effect are almost always polar, the need for a high concentration of NLO chromophore may reduce the ultimate mobility in some cases.

Third, the second-order nonlinearity must be induced in the polymer by applying an electric field to align the chromophores and remove the center of symmetry which would be present in a random distribution. The alignment of the molecules can be either permanent (actually quasipermanent), in which case the molecules remain aligned after the field is removed, or temporary, in which case the molecules remain aligned only as long as the field is applied to the material. The scheme used most often for achieving stable poling is to heat the material to a temperature near the glass transition temperature T_g, apply an electric field to the material, cool the material to a temperature well below T_g, and then remove the field. At this lower temperature, the molecules are unable to easily relax back to a random distribution of orientations. Much work has been done on the poling process to maximize both the value of the electrooptic coefficient and its stability;[44] for example, cross-linking has been used during poling to achieve larger net alignment at the same time that T_g is increased. However, if the T_g of the material is sufficiently low such that the NLO chromophores can be oriented at room temperature, the value of r_e is a function of the applied field and is generally observed to be linearly proportional to the field since saturation of the orientation is seldom reached. This is the situation with many of the PR polymers studied so far, and due to a novel enhancement effect,[45] the ability of the NLO chromophores to orient at ambient temperatures is actually an advantage (see section IV.C).

The nature of the trapping sites in photorefractive materials is only rarely known in detail. For example, several decades of detailed studies on $BaTiO_3$ were necessary[46] in order to reach the present understanding of the trapping centers, which are most likely oxygen vacancies and Fe^{n+} ions. It is generally agreed that the deep traps in the inorganic crystals are either vacancies, interstitials, or impurities with multiple valence states. For all of the PR polymers reported in this review, no additional trapping components were added. Since the PR polymers are a relatively new class, it is not surprising that the nature of the traps is not well-known, but some general comments can be made. Since the transport usually occurs via a network of transport molecules in an amorphous host with configurational disorder, there should be a distribution of energies for carriers, the tail of which provides a set of shallow traps which empty thermally. Measurements on specific PR polymers providing evidence for the existence of shallow traps are presented in section III. Deeper traps could result from molecules or ionic impurities with several stable oxidation states, and the location of the relevant energy levels for deep traps is discussed in the next section. For a few PR polymers, the trap density has been estimated and found to be on the order of 10^{15} to 10^{16} per cm^3 (see section III), values which are roughly

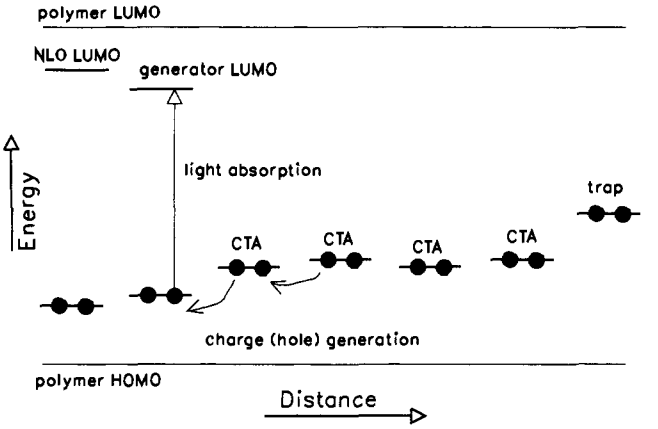

Figure 2. Schematic illustration of the location of the relevant energy levels for the various components of a PR polymer in the context of hole generation, transport, and trapping processes. The HOMO–LUMO optical absorption of the host polymer, NLO chromophore, and charge generating agent must be at longer and longer wavelengths, respectively. The charge-transport agent (CTA) is not optically excited, but forms a network for hopping of photogenerated holes to a trapping site.

comparable to those for inorganics.[47] It is clear that further study and optimization of the trapping centers in PR polymers using techniques like ESR and thermally stimulated currents are needed, especially since the density of traps controls the maximum space–charge field that can be generated and the maximum spatial information that can be recorded in the hologram.

C. Measurements of Required Properties

1. Optical Absorption, Regions of Transparency

Since the desired action of the light beam on the PR material is generation of mobile charge, it is an obvious first requirement that the material have optical absorption at the operating wavelength. In fact, the absorption properties of the various components of a PR polymer must be chosen carefully in order to optimize the PR behavior, especially since both the NLO chromophore and the charge-transporting molecule are usually present in high concentration to maximize optical nonlinearity and charge transport, respectively. It should be noted that optical experiments on inorganic PR crystals are generally performed at long wavelengths, in the optical bandgap, with most of the effects controlled by the optical absorption of impurity or defect levels within the gap. To describe the corresponding situation in organics, the optimal ordering of the energy levels (especially the energy differences between the HOMO and LUMO) of the various components of a PR polymer mixture is shown in Figure 2, and the optical absorption of a particular PR polymer mixture is shown in Figure 3. Most host polymers (either those which photoconduct or those to which NLO chromophores are attached) are transparent in the visible, so the HOMO–LUMO transition of the inert portion of the host is often in the ultraviolet.

Most NLO chromophores are strongly absorbing in the blue and green portions of the visible, because high nonlinearities derive from the close proximity of a strong charge-transfer transition.[44] It is necessary for the charge-generating agent to have the smallest optical

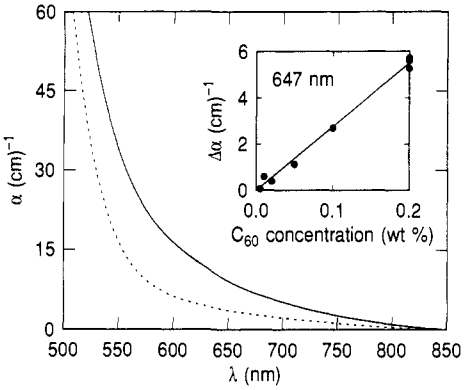

Figure 3. Absorption coefficient α as a function of λ for PMMA-PNA:DEH undoped (dashed line) and doped with 0.2 wt % C_{60} (solid line). The inset shows the change in absorption due to C_{60} as a function of concentration at 647 nm. (Reprinted from ref 79. Copyright 1992 American Institute of Physics.)

gap and therefore the longest wavelength absorption, so that the optical wavelength can be chosen to minimize the absorption by all components except the charge generator. This assures that the light is preferentially absorbed by the charge-generating molecules, which is the optimal situation for the PR effect. Absorption by any of the other components will increase the background absorption and not contribute to the PR effect. Such wasted absorption should be avoided in order to (i) minimize the production of competing photochromic gratings, and (ii) minimize the amount of absorption which competes with 2BC gain (discussed in section II.E). In particular, the optical absorption of the charge-transporting agent (CTA) should be of high energy, thus the LUMO is not shown in Figure 2. In order to allow optical erasure, it is useful to have the trap molecule absorb light when it contains a charge carrier, but this is also not shown in figure for simplicity.

Figure 2 also illustrates the necessary ordering of the HOMO's of the various components of the PR polymer (for the case in which holes are the mobile charge carriers). The relative locations of the energy levels can be determined with ionization potential and electron affinity measurements, but these techniques may not be easily applied to a PR polymer mixture. Reference to the literature on electron-transfer photosensitization[48] provides an alternate method for determining the relative ordering of the levels. With certain assumptions about solvent stabilization and polarization energies, the relative ordering of the HOMO's of the various components can be estimated electrochemically and discussed in terms of the oxidation potential E_{ox} of the molecule, which is the energy required to remove an electron from the molecule relative to a standard electrode in a fixed solvent and electrolyte. The charge-transporting (CTA) molecules (for example, DEH molecules) form a connected network throughout the polymer so transport can occur by hopping from molecule to molecule. In order for it to be energetically favorable for the optically excited charge-generating molecule to donate a hole to the charge-transporting network, E_{ox} of the generator must be larger than that of the CTA. It is also important that E_{ox} of the NLO chromophore be larger than that of the charge-transporting molecule, or the NLO chromophore will act as a trap which is present in such high densities as to destroy the photoconductivity of the material entirely. Any intentionally added trapping molecules will only provide deep traps if E_{ox} for the trap is less than E_{ox} of the CTA by more than k_BT, where k_B is Boltzmann's constant and T is the temperature. As a final remark, for hole transport, the generator is photoreduced and the trap is oxidized during grating formation.

To give a concrete example of these considerations, the absorption spectrum of the photorefractive polymer PMMA-PNA:DEH (discussed in sections III.A.2.b and III.A.3) is shown in Figure 3, both undoped (dashed line) and doped with 0.2 wt % of the generator molecule C_{60} (solid line). The sharp increase in absorption below 550 nm in the undoped sample is due to absorption by the nonlinear PNA chromophore, and the tail of the absorption extending beyond 650 nm is due to a weak charge-transfer complex formed between the PNA and the CTA molecule, DEH. The addition of the generating agent (or sensitizer) C_{60} increases the absorption of the material at wavelengths larger than 550 nm. The increase in the absorption coefficient α at 647 nm is shown as a function of C_{60} concentration in the inset of Figure 3. The effect of C_{60} as a sensitizing agent in PMMA-PNA:DEH is discussed in section III.A.3.

2. Transport Properties

Since the transport properties of PR polymers are sufficiently different than that for inorganic PR crystals (see section II.B), measurement of these properties is an important first step in the characterization of a potential PR polymer. The central parameter governing the charge transport is the photoconductivity, σ_{ph}, which may be written for the case of mobile holes

$$\sigma_{ph} = pe\mu = (\phi\alpha I\tau_{eff}/h\nu)e\mu \qquad (3)$$

with p the density of mobile holes produced at intensity I, e the elementary charge, ν the optical frequency, h Planck's constant, and μ the (hole) mobility. The effective carrier lifetime τ_{eff} is controlled by recombination and trapping processes (see section IV). One detailed study of the transport properties of a PR polymer has been presented[39-41] in which σ_{ph}, μ, and ϕ were all measured, and this work should be consulted for details of the experimental techniques. The photoconductivity can be measured by a simple dc technique in which the current is measured in the absence and presence of an excitation beam, and the result expressed in terms of a conductivity change per unit light intensity. Values in the range 10^{-14} to 10^{-9} $(\Omega\text{-cm})^{-1}/(W/cm^2)$ are common for PR polymers depending upon the value of α at the wavelength of excitation. A superior method is the xerographic discharge technique,[39] which measures the rate of discharge of a leaky capacitor formed by the sample both in the absence and presence of light. Such xerographic discharge measurements, although more difficult experimentally, yield more reliable results. In all cases, true photogeneration must be distinguished from an increase in dark conductivity due to heating. The quantum efficiency of charge generation can be determined by a straightforward analysis of the photoconductivity.

The mobility can be measured by the standard time-of-flight technique in a thin-film capacitive geometry.[49] Using wavelengths in the ultraviolet which are strongly

absorbed in a thin layer of order 100 nm, a sheet of charges are created in the sample adjacent to the illuminated electrode. The carriers propagate across the sample under the influence of an applied electric field, and the mean transit time τ_T is obtained by appropriate averaging of the drop in the current which signals the arrival of the carriers at the second electrode.[50] Knowledge of the applied field, sample thickness, and τ_T allows calculation of μ. Such measurements have been performed in detail for many molecularly doped polymers used in the electrophotographic industry.[33-38]

To give examples of measured transport parameters for selected PR polymers, the (specific) photoconductivity of the PR polymer bisA-NPDA:DEH was determined[39] to be 10^{-12} to 10^{-11} $(\Omega\text{-cm})^{-1}/(W/cm^2)$ for wavelengths near 650 nm and fields near 40 V/μm. The observed mobility values were in the range 10^{-7} to 10^{-6} cm^2/V s, and the quantum efficiencies of charge generation approached 10^{-2}. In a doped poly(silane), however, much larger mobilities were observed,[43] approaching 10^{-3} cm^2/V s at 40 V/μm, which was 1 order of magnitude larger than the undoped poly(silane) value. Other transport measurements will be discussed in sections III and IV.A.

3. Electrooptic Response

A number of different methods have been developed to measure the electrooptic coefficient in polymer films. The most commonly used method for thick polymer films is a Mach–Zehnder interferometric technique.[51,52] A sample is mounted in one arm of an interferometer on a rotation stage which varies the angle of incidence, and the incoming beam is polarized perpendicular to the axis of rotation of the sample (i.e., s-polarized). The voltage applied to the sample consists of (in the most general case) two components: an ac voltage, typically 20–100 V (rms) with a frequency f ranging from 1 to 100 kHz, and a dc bias voltage of up to 10 kV. The phase shift induced by the ac field is measured using a lock-in amplifier to detect a power modulation in the beam exiting the interferometer at the fundamental frequency f of the ac field (or harmonics of f). From this phase shift, the change in index of refraction and the electrooptic coefficient(s) can be computed. Reflectance[53,54] and attenuated total reflection (ATR)[55] techniques have also been used to measure r in thin poled polymer films, and a heterodyne detection technique[56] has been used to measure r in films in a wave-guide geometry.[57]

In all cases, what is actually measured is the variation in optical path of the sample as the electric field is modulated. This means that changes in either the optical index of refraction (the desired effect) as well as changes in the sample thickness contribute to the observed signal. A noncentrosymmetric material can have not only a nonzero electrooptic coefficient but also a nonzero piezoelectric coefficient.[58] Piezoelectric resonances of the sample that can occur at low frequencies must be avoided in the determination of the electrooptic coefficient, and in some cases separate measurement of the piezoelectric coefficient is required.[59] Moreover, in the presence of a dc bias field, a variety of quadratic electrooptic effects[60] can mimic a linear electrooptic response and must be considered as a source of the observed signal. The values of the electrooptic coefficients observed for various PR polymers will be discussed in section III.

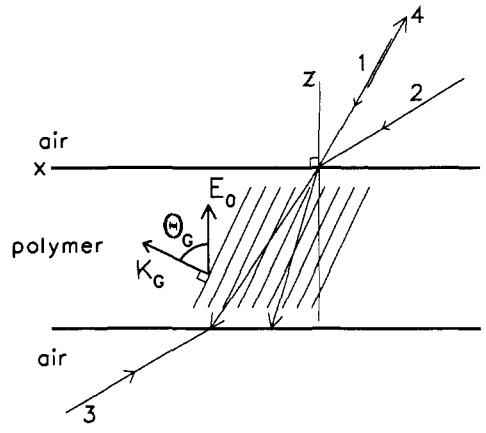

Figure 4. Experimental geometry for the PR grating experiments. The grating is written by beams 1 and 2, which enter the sample with angles θ_1 and θ_2 (all angles are defined with respect to the sample normal inside the sample). The grating is written at a wave vector K_G, with an angle θ_G to the external electric field E_0. For the FWM experiments, the grating is probed with beam 3, which is collinear and counterpropagating to beam 2. The diffracted beam appears collinear and counterpropagating to beam 1. (Reprinted from ref 61. Copyright 1991 Society of Photo-Optical Instrument Engineers.)

D. Four-Wave Mixing Grating Measurements

Although the necessary elements of photorefractivity discussed above may be measured to be nonzero in a given organic polymer or polymer mixture, the presence of the PR effect must be demonstrated by writing gratings in the material. In particular, the dominance of the PR effect over other competing sources of gratings (such as photochromism) must be demonstrated. Gratings can be conveniently written and read out in a material using several holographic optical techniques, and here we describe the most common method used for PR polymers, four-wave mixing (FWM). Two mutually coherent writing beams of the same polarization (s- or p-polarized) are spatially overlapped in the polymer film, with an angle $2\theta_0 = \theta_2 - \theta_1$ between them. (If the beams are pulsed, they must be temporally overlapped as well.) Assuming the NLO chromophores in the sample are aligned along the sample normal, the normal of the sample must be rotated with respect to the bisector of the write beams[17,61] to provide a nonzero r_e along the grating wave vector $\vec{K}_G$. In addition, this oblique geometry provides a nonzero component of the externally applied dc field along $\vec{K}_G$ to enable drift of the photogenerated charge carriers in the direction of $\vec{K}_G$. This geometry is shown in Figure 4, with an external angle of 30° between the writing beams and the sample tilted 45° with respect to the sample normal. These are the typical conditions for many of the experiments discussed below.

In the FWM experiments a much weaker read beam can be used to probe the grating in the phase-conjugate geometry. In all of work discussed in this paper, the reading beam is the same wavelength as the writing beams and is counterpropagating to one of the write beams (degenerate FWM geometry). The read beam

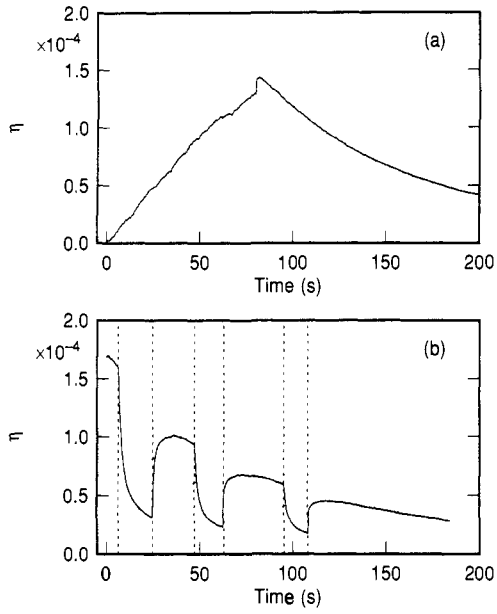

Figure 5. Illustration of the grating dynamics in the PR polymer bisA-NPDA:DEH (λ = 647 nm, E_0 = 11.4 V/μm). (a) The writing beams are turned on at t = 0 and the diffraction efficiency η grows with a response time of several tens of seconds. At t = 80 s the writing beams are turned off and the grating decays slowly in the presence of the reading beam only. Part b shows electric field dependence of η during reading. The field which was present during writing is turned off at 6.4 s and η quickly decays by a factor of 4, due to randomization of the alignment of the chromophores. At t = 25 s the field is turned back on and η increases as the chromophores reorient. This cycle is repeated at t = 47 s and t = 95 s.

is diffracted by the grating with an efficiency η, defined as the intensity ratio of the diffracted beam to the incoming read beam. The diffracted beam is directed into a detector as a background-free signal, which allows very small signals (very weak gratings) to be detected. Of course, it would also be possible to probe the gratings by blocking one writing beam and observing the diffraction of the other writing beam, but this method does not allow recording of η as a function of time during the writing process.

The first piece of evidence that a grating written in a polymeric material is photorefractive in origin is the dynamic behavior of the grating. This is shown in Figure 5 for the polymer mixture bisA-NPDA:DEH (a material discussed in detail in section III.A.1.a) with an applied field of E_0 = 11.4 V/μm. Figure 5a shows the growth of the diffraction efficiency as the writing beams are turned on at t = 0. The diffraction efficiency grows slowly over the 80-s writing time. At t = 80 s, the writing beams are blocked, and the diffraction efficiency decays in the presence of the reading beam with a time constant on the order of 100 seconds. Figure 5b shows the field dependence of η during reading. At t = 6.4 s, the field is turned off (E_0 = 0 V/μm) and the diffraction efficiency decreases rapidly by a factor of 4. η increases significantly again as E_0 is switched back on at t = 25 s. This field cycling is repeated again at t = 47 and t = 95 s. η decreases as the field is removed from the sample due to the relaxation of the chromophore orientation, as the sample is not permanently poled due to the low T_g. The issue of chromophore orientation is discussed in detail in sections III and IV.

The space-charge field E_{sc} remains stored in the material however, so η increases again as the external field is restored. On a longer time scale, E_{sc} also decays due to dark conductivity and photoconductivity induced by the reading beam.

It is important to realize that field-dependent gratings alone are not sufficient evidence to establish that the PR effect is operative. Many photochemical reaction mechanisms can be enhanced by an applied electric field and would produce field-dependent diffraction grating formation. In addition, if photochemistry produces spatially modulated density, electroabsorption and electrorefraction effects can produce diffracted signals depending upon the applied electric field. An additional piece of evidence that field-dependent gratings are photorefractive in origin can be obtained from the polarization anisotropy of the FWM signal during readout. After writing with both beams p-polarized or both beams s-polarized, one may consider how the diffraction efficiency depends upon the polarization of the reading beam. The symmetry of the electrooptic tensor in a poled polymer[62] controls the polarization anisotropy during readout. For the $C_{\infty v}$ symmetry, only the coefficients r_{33} and $r_{13} = r_{23} = r_{42} = r_{51}$ are nonzero. For the general case of oblique readout from tilted PR phase gratings,[21,61] the diffraction efficiencies for s- and p-polarized readout are (for a Δn grating due to the simple electrooptic effect; for modifications to this anisotropy due to the orientational enhancement effect, see section IV.C)

$$\eta_s = \sin^2\left[\frac{\pi n^3 r_{13} E_{sc} d \cos\theta_G}{2\lambda_v(\cos\theta_2 \cos\theta_1)^{1/2}}\right] \quad (4)$$

$$\eta_p = \sin^2\left[\frac{\pi n^3 r_e^p E_{sc} d \cos(\theta_2 - \theta_1)}{2\lambda_v(\cos\theta_2 \cos\theta_1)^{1/2}}\right] \quad (5)$$

where d is the sample thickness and θ_G the angle between the grating wave vector and the film normal (see Figure 4). (Note that in previous work,[61] eqs 4 and 5 were expressed in terms of the complementary angle θ_g, the angle between the grating wave vector and the film plane. To be consistent with more recent work[45] we define all angles with respect to the film normal.) For the geometry shown in Figure 4 and assuming a polymer index of refraction of 1.7, θ_1 = 18.4°, θ_2 = 33.1°, and θ_G = 64.2°. The effective EO coefficient for p-polarized readout is given by[61]

$$r_e^p = r_{13}[\cos\theta_1 \sin(\theta_G - \theta_2) + \sin\theta_1 \cos\theta_2 \sin\theta_G] + r_{33} \sin\theta_1 \sin\theta_2 \cos\theta_G \quad (6)$$

which for the angles in use here gives $r_e^p = 1.3r_{13}$ using the standard assumption for linear chromophores and weak poling of $r_{33} = 3r_{13}$.[62] Equations 4 and 5 therefore predict a readout polarization anisotropy ratio of η_p/η_s = 8.3 for a photorefractive grating. Even though measurement of a polarization anisotropy near this value is suggestive of a PR grating, it is still possible that another grating formation mechanism fortuitously produced the anisotropy. In practice, it is much more convenient and conclusive to utilize the presence of asymmetric two-beam coupling as the definitive test for photorefractivity.

E. Two-Beam Coupling Gain—A Simple Test for Photorefractivity

In order to unambiguously distinguish between the PR effect and other types of gratings which may occur in polymers, two-beam coupling (2BC) measurements must be performed. In the 2BC experiments the change in the transmitted intensity of either of the write beams is recorded as the other write beam is switched on and a grating is formed. Each write beam is partially diffracted in the direction of the other write beam by the grating. By monitoring the intensity of both writing beams as the grating is formed, the nature of the grating can be determined. This is done most clearly when the intensities of the two writing beams are equal (before the sample). There are three possible cases: (i) Symmetric loss (gain) in both of the writing beams is the signature of an increase (decrease) in the absorption coefficient which is in phase with the intensity grating. Such in-phase absorption gratings can result from many processes[10] such as photochemistry, excited-state population, electronic $\chi^{(3)}$, and thermal effects. (ii) No change in the intensity of the writing beams is the result of either an in-phase index of refraction grating or a 90° phase-shifted absorption grating. (iii) An asymmetric change in the intensities of the two writing beams, i.e., an increase of intensity of one of the writing beams and an approximately equal decrease in the intensity of the second writing beam can only occur from an index of refraction grating which is phase shifted relative to the intensity grating. Thus, the asymmetric change of intensity of the two writing beams as the grating is written is a clear signature of the PR effect.

From the increase in intensity of the transmitted beam with gain, it is possible to directly determine the beam-coupling ratio $\gamma_0 = P_{\text{signal,with pump}}/P_{\text{signal,without pump}}$, where P_{signal} is the measured power (after the sample) of the write beam under consideration. The normalized beam-coupling gain coefficient Γ (more precisely, the energy-transfer coefficient) is given in terms of the measured quantities γ_0 and β, the ratio of the write powers before the sample, as[27]

$$\Gamma = \frac{1}{L}[\ln(\gamma_0\beta) - \ln(\beta + 1 - \gamma_0)] \qquad (7)$$

where $L = d \cos\theta$ is the optical path for the beam with gain, and the effects of obliquity, i.e. different path lengths, total absorption, and reflection losses for the two beams have been neglected. Net internal gain is achieved in the material when Γ exceeds the absorption coefficient α of the material ($\Gamma - \alpha > 0$). To realize net gain in one beam for a practical application, beam ratios $\beta \gg 1$ should be used (undepleted pump regime). The necessity of two-beam coupling gain for certain applications of PR materials was discussed in section II. In practice, $(\Gamma - \alpha)L > 1$ is often required.

As a specific example, Figure 6 shows the normalized intensity $I/I(t=0)$ of both writing beams measured in a 2BC experiment for the PR polymer mixture PVK:PDCST:TNF (discussed in detail in section III.B.) at $E_0 = 32$ V/μm with $\beta = 1$. The figure shows the results of two separate experiments. In the first experiment, the intensity of beam 1 is monitored as beam 2 is switched on at $t = 0$ and switched off at $t = 120$ s (open circles). In the second experiment, the intensity of beam 2 is monitored as beam 1 is switched on at $t = 0$ and

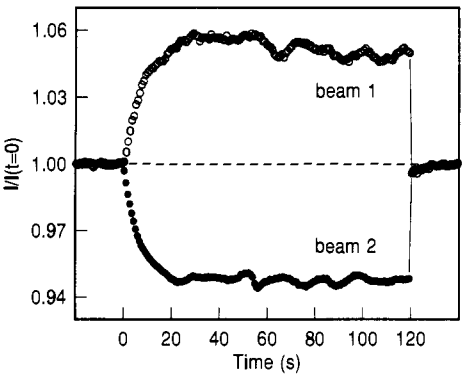

Figure 6. Two-beam-coupling experiment for PVK:PDCST:TNF at 753 nm with $E_0 = 32$ V/μm and $\beta = 1$. The intensity of beam 1 is monitored as beam 2 is switched on at $t = 0$ and off at $t = 120$ s (open circles) and the intensity of beam 2 is monitored as beam 1 is turned on at $t = 0$ and off at $t = 120$ s. The asymmetric energy transfer is proof of the photorefractive origin of the grating. (Reprinted from ref 89. Copyright 1993 Optical Society of America.)

switched off at $t = 120$ s (filled circles). As the grating is written, the intensity of beam 1 increases and the intensity of beam 2 decreases by an approximately equal amount, indicating an index-of-refraction grating which is spatially phase-shifted relative to the light intensity grating. From the saturation value of $I/I(t=0) = \gamma_0 = 1.06$ for beam 1, a 2BC gain coefficient of $\Gamma = 7.8$ cm^{-1} is calculated. This exceeds the measured absorption coefficient α of the material (2.3 cm^{-1}) and therefore net internal gain is observed in PVK:PDCST:TNF.

The contributions to the optical response due to absorption and refractive index modulation as well as the phase of each of the contributions can be determined by a grating translation technique developed by Sutter and Günter,[16] modified to include the effects of p-polarized readout in the oblique geometry[63] of Figure 4. This can be accomplished either by changing the relative phase of the two writing beams, resulting in a shift of the interference pattern in the sample, or by translating the position of the sample while the interference pattern remains fixed. In either case, the grating translation rate should be significantly faster than the growth rate of the grating to be measured. This technique has been applied to the bisA-NPDA:DEH material which will be discussed in section III.A.1.a.

III. Materials Classes

The necessary elements of photorefractivity are photoinduced charge generation, charge transport, trapping, and electrooptical nonlinearity. Therefore a polymeric material can potentially be made photorefractive either by incorporating these properties directly into the polymer or by doping guest molecules into the polymer to produce these properties. It is usually desirable to incorporate at least some of the PR properties into the polymeric host itself to minimize the amount of inert volume in the material.

The schematic drawings in Figure 7 show three approaches to providing the required functionality which have been investigated to date. The first class illustrated in Figure 7a consists of an optically nonlinear polymer with nonlinear optical (NLO) moieties covalently bonded to the polymer backbone, either as side-chain or main-chain substituents. An alternative

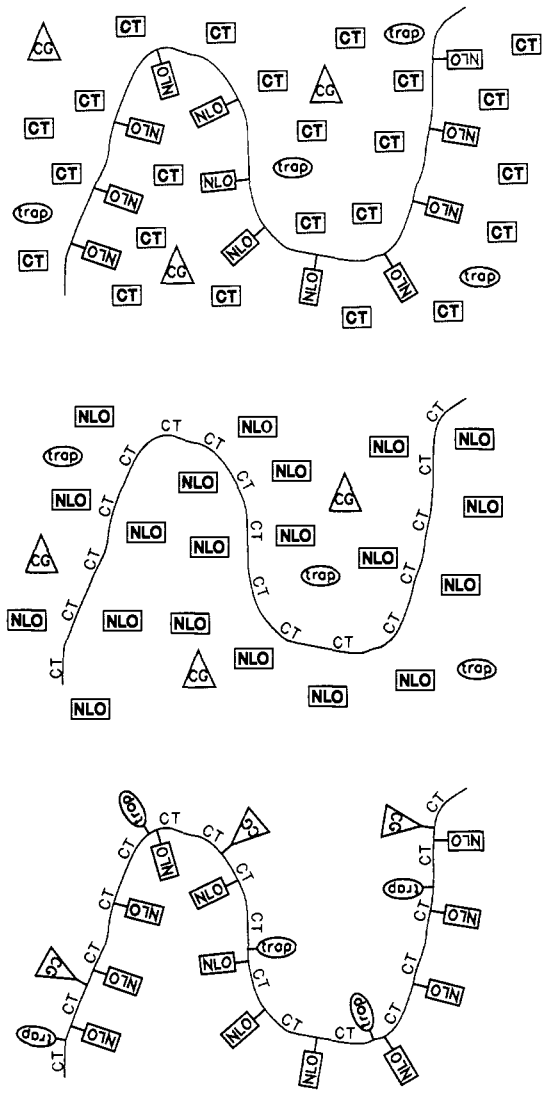

Figure 7. Different approaches to creating a photorefractive polymeric material. (a) The nonlinear optical (NLO) property is incorporated into the polymer, while the functional groups responsible for charge generation (CG), charge transport (CT), and trapping are incorporated as guest molecules in the polymer matrix. (b) The CT occurs along the polymer chain and the remaining functionalities are incorporated as guests in the matrix. (c) The functional groups responsible for all of the necessary elements are attached to the polymer backbone.

approach to providing the optically nonlinear host polymer already familiar from the work on inorganics[64-68] would be to utilize a $\chi^{(3)}$ polymer such as poly(*p*-phenylenevinylene) in a bias electric field to produce the required (second-order) optical nonlinearity. In either case, the nonlinear host material is doped with small molecule charge transport agents (CT) in concentrations high enough to ensure bulk transport of the photogenerated charges by hopping from transport molecule to transport molecule, as is well known in the electrophotographic industry.[69] Charge generation and trapping may be provided by the NLO polymer itself. Alternatively, the PR response can be optimized by including additional dopants in relatively low concentration to perform the functions of charge generator (CG) or traps. Various charge generating dyes and pigments (sensitizing agents[70]) are known in the fields of photography and electrophotography. PR polymers of this general type are described in section III.A.

The second approach to producing a PR polymer is shown in Figure 7b. In this case, the host material consists of a charge transporting polymer which contains charge transporting groups (CT) either as main-chain or side-chain substituents on the polymer backbone. The material is made to be optically nonlinear by the addition of an NLO chromophore in as high a concentration as possible to maximize the optical nonlinearity upon poling. As in the first class, additional dopants can be added to provide or improve charge generation (CG) and trapping. Examples of materials of this type are described in section III.B.

A third approach to producing a PR polymer involves covalent attachment of all the required functionalities directly to the polymer backbone, referred to as fully functionalized polymers (Figure 7c). To date, several potential materials of this type have been reported, but the performance has been inferior to that for the other two materials classes. Materials of this type will be discussed in section III.C.

A. Doped Materials Based on Nonlinear Optical Polymer Hosts

Photorefractive polymers have been reported using three distinct types of NLO polymer hosts. The first type of host polymer is one in which the NLO chromophore is cross-linked into an epoxy material through multiple bonds between the epoxy chains and the NLO chromophore. The second type of polymer is a copolymer of methyl methacrylate and an acrylate which has been derivatized with the NLO chromophore which results in the NLO chromophore appearing as a pendant group attached to the polymer backbone. A third type of NLO polymer that has been utilized is a linear epoxy, where the NLO chromophore is attached as a side group on an epoxy backbone. All of the NLO polymers-charge transport agent–sensitizer combinations in which photorefractivity has been reported are listed in Table 2, along with values of some of their photorefractive parameters. The structures of all of the NLO polymers are shown in Figure 8, and the structures of the CT agents and charge-generating sensitizers are shown in Figure 9. All of these materials are discussed in detail in this section.

It is worth noting that many other types of polymers have been (or are currently being) developed for purely nonlinear optical applications, such as electrooptic modulators and devices for generating frequency-doubled laser light.[44] These include polymers in which the NLO chromophore is incorporated into the polymer backbone, and cases in which the chromophore is attached at both ends to the polymer matrix. The goal of this related work is to maximize the second-order optical nonlinearity of these polymers, usually by maximizing the molecular nonlinearity and the order parameter which measures the degree to which the chromophores are aligned. Many of these NLO polymer materials could also potentially serve as PR polymer hosts, as the modulation of the index of refraction due to electric fields is also proportional to the second-order optical nonlinearity (cf. eq 2).

1. Cross-Linked Epoxy Hosts

Two examples of this type of PR polymer are shown in Table 2, both of which are formed by reaction of a

Table 2. Optical Properties of Doped Materials Based on NLO Polymer Hosts

NLO polymer	CT agent[a]	sensitizer[b]	λ (nm)	α (cm^{-1})	η_{ss}[c]	τ (s)[d]	Γ (cm^{-1})[e]
bisA-NPDA[17,61]	DEH	none	647	10	5×10^{-5} [e]	100[f]	0.33
bisA-NPDA[61]	DENH	none	647	10	1×10^{-5}		
bisA-NPDA[61]	DECH	none	647	10	9×10^{-5}		
NNDN-NAN[61]	DEH	none	647		1×10^{-3} [g]		
PMMA-PNA[72]	DEH	none	568	5.9	1×10^{-5}	2	0.23
			647	1.1	4.9×10^{-6}	7	0.11
PMMA-MSAB[77]	TTA[h]	BDK[i]	633	75	3.2×10^{-5} [j]		
PMMA-PNA[79,80]	DEH	C_{60}[k]	647	3.4	4.8×10^{-5}	0.25	0.6
PMMA-PNA[80]	DEH	TNF	647	3.2	1.1×10^{-5}	10[h]	
PMMA-PNA[80]	DEH	squaryllium	647	12	1.8×10^{-5}	28[l]	
PMMA-PNA[80]	DEH	anthracene-TCNQ	647	25	3.3×10^{-5}	2.3[l]	
PMMA-PNA[80]	DEH	p-dci	647	2.0	6.7×10^{-5}	9.0[l]	
			647	40	8×10^{-6} [m]	0.16	2.2[m]
bisA-NAT[80]	DEH	none	676	18			1.8[m]
			753	2.4			1.2[m]
bisA-NAT[83]	DEH[n]	none	650	118	1.1×10^{-2} [o]		

[a] CT agent concentration 30 wt %, unless otherwise noted. The structures and complete names are given in Figure 9. [b] Sensitizer concentration 0.1 wt %, unless otherwise noted. The structures and complete names are given in Figure 9. [c] Sample length 350 μm, E = 11 V/μm, unless otherwise noted. [d] Intensity 1 W/cm^2, unless otherwise noted. [e] E = 12.5 V/μm. [f] Intensity 13 W/cm^2. [g] E = 8.5 V/μm. [h] 31 wt %. [i] 0.03 wt %. [j] Sample length 300 μm, E = 32.5 V/μm. [k] 0.2 wt %. [l] Estimated τ, see ref 80. [m] Sample length 36 μm, E = 55 V/μm. [n] 40 wt %. [o] Sample length 145 μm, E = 13.8 V/μm.

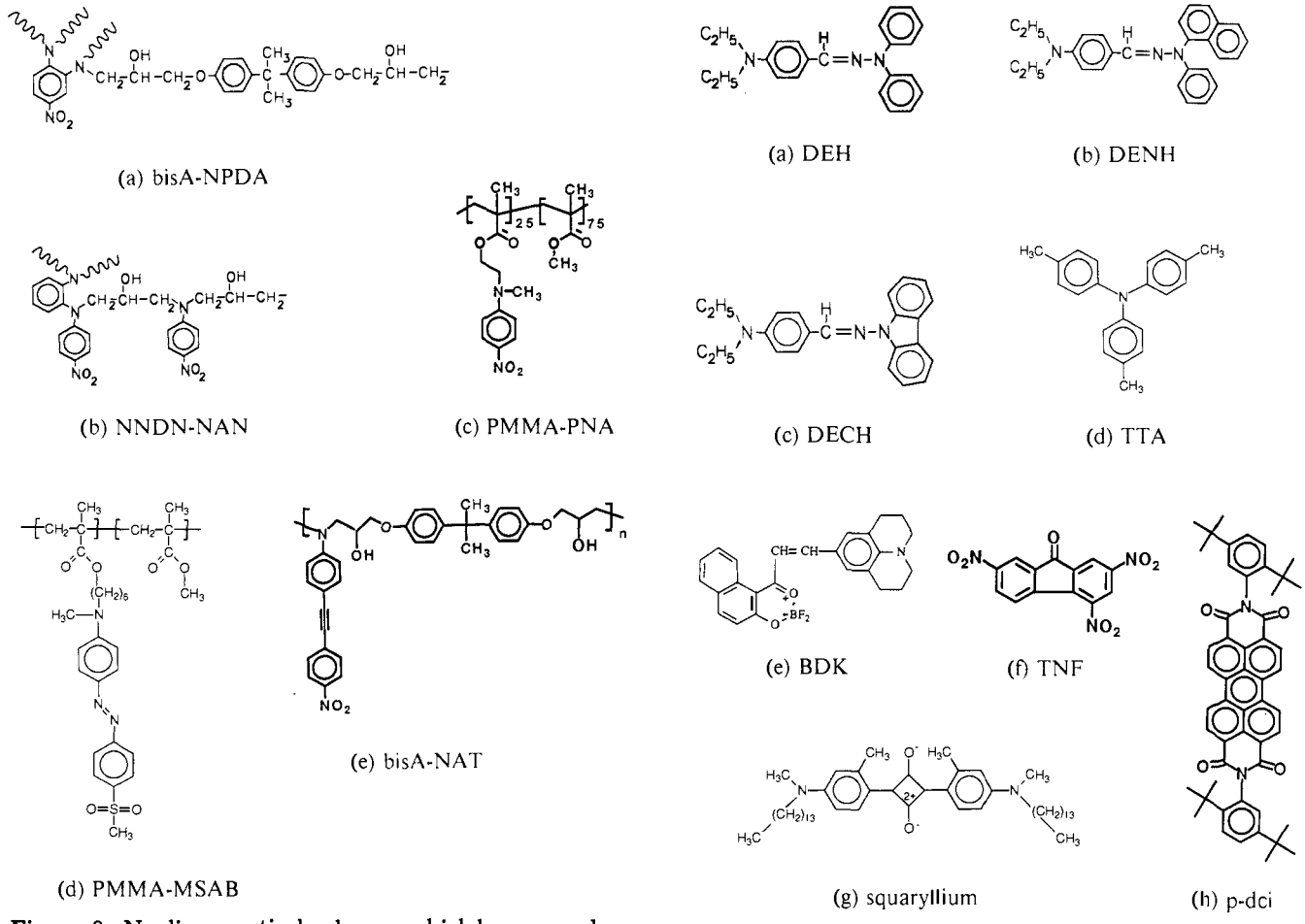

Figure 8. Nonlinear optical polymers which have served as hosts for photorefractive polymers. The origins for each of the acronyms are given in the text.

Figure 9. Charge-transporting molecules which have been added to the NLO polymers: (a) (diethylamino)benzaldehyde diphenylhydrazone (DEH); (b) *p*-(diethylamino)benzaldehyde *N*-(1-naphthyl)-*N*-phenylhydrazone (DENH); (c) *N*-[[4-(diethylamino)phenyl]methylene]-9*H*-carbazol-9-amine (DECH); and (d) tritolylamine (TTA). The following are charge-generating sensitizers which have been added to the NLO polymer:charge transporting molecule mixtures: (e) boron diketonate (BDK); (f), 2,4,7-trinitro-9-fluorenone (TNF); (g) a solubilized squaryllium dye; and (h) *N,N'*-bis-(2,5-di-*tert*-butylphenyl)-3,4:9,10-perylenebis(dicarboximide) (p-dci).

bisepoxide with NLO chromophores containing primary or secondary amines.

a. bisA-NPDA:DEH. The first proven PR polymer, bisA-NPDA:DEH, was reported[14,17] in 1990, which attests to the relative youth of this entire field. The bisA-NPDA host polymer (Figure 8a) was formed by thermally reacting the bifunctional monomer bisphenol A diglycidyl ether (bisA) with the trifunctional non-

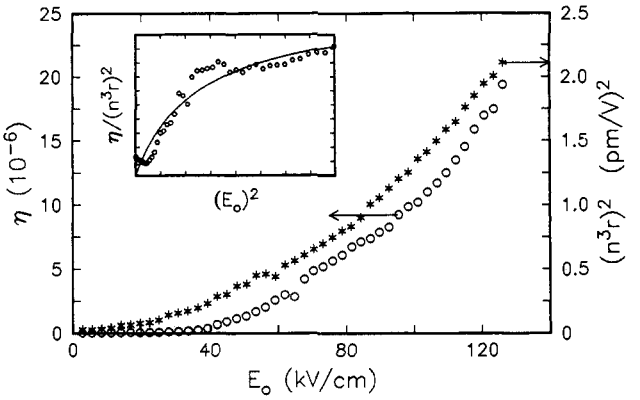

Figure 10. Photorefractive and electrooptic response of bisA-NPDA:DEH. The right ordinate is the square of the electrooptic response (n^3r_e, with n the index of refraction) for p-polarized 633-nm radiation incident at an external angle of 60° on a 356-μm film. The left ordinate is steady-state diffraction efficiency η_{ss} at 647 nm (3 W/cm^2 writing intensity, 750-μm beam diameter) for the same sample as a function of the applied field. The inset shows the ratio of the latter to the former, which is proportional to E_{sc}^2. (Reprinted from ref 17. Copyright 1991 American Institute of Physics.)

linear chromophore 4-nitro-1,2-phenylenediamine (NPDA). The presence of two reactive amines on the chromophore resulted in a cross-linked nonlinear polymer with the useful property of improved stability of the optical nonlinearity.[18] Monopolar (hole) charge transport was provided by doping the polymer with the well-known[71] charge-transport agent, (diethylamino)benzaldehyde diphenylhydrazone (DEH; Figure 9a) at a concentration of 30 wt %. No explicit traps or charge-generating agents were added to the bisA-NPDA:DEH mixture. The NPDA chromophores, which have a weak absorption at the 647-nm wavelength at which the experiments were performed, acted as the charge generators, and the traps were assumed to be inherent in the polymer. Due to the partial crosslinking and low T_g of the polymer (65 °C; further depressed by the presence of DEH), the chromophores could be oriented at room temperature, and all experiments were done in the presence of an applied field E_0. The PR properties of bisA-NPDA doped with two other hydrazone-based charge transport agents, DENH (Figure 9b) and DECH (Figure 9c), have also been reported[61] (see Table 2).

The PR effect was first established in bisA-NPDA:DEH by using FWM to investigate the dynamic behavior, field dependence, and polarization anisotropy η_p/η_s of gratings written in the sample.[17] As with almost all of the PR polymers reported to date, the sample investigated was composed of the polymeric material (cast from solution) sandwiched between two glass plates coated with indium–tin oxide (ITO), an optically transparent conductive material which allows an electric field to be applied across the sample. The thickness of the polymer layer was 350 μm. The dynamic behavior of the diffraction efficiency was shown in Figure 5 above. As discussed in the previous section, the dynamic properties of the grating are consistent with the PR effect. The steady-state diffraction efficiency η_{ss} is shown as a function of applied field E_0 for bisA-NPDA:DEH in Figure 10. As E_0 is increased η_{ss} increases, from $<10^{-6}$ (detection limit) to a maximum value of 2×10^{-5} at $E_0 = 12.6$ V/μm. The square of the effective

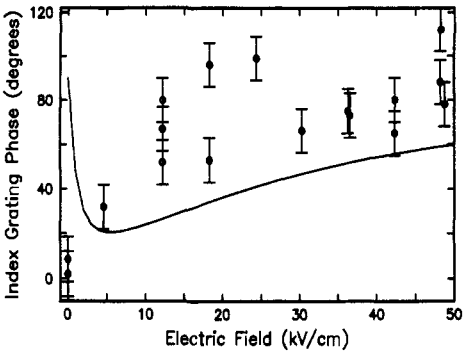

Figure 11. The spatial phase shift of the index grating (relative to the intensity grating) as a function of applied electric field along the grating wavevector in bisA-NPDA:DEH. At zero field the phase shift is near zero, indicating a nonphotorefractive grating. As the field increases, the phase of the index grating increases to 90° as the photorefractive grating becomes dominant. The solid line is the phase shift expected from the standard PR model. (Reprinted from ref 63. Copyright 1992 Optical Society of America.)

nonlinear coefficient of the sample n^3r_e is also shown as a function of applied field in Figure 10.

The inset to Figure 10 shows $\eta_{ss}/(n^3r_e)^2$, which should be proportional to the square of the space-charge field E_{sc} in the standard PR theory, (cf. eq 5) plotted as a function of $(E_0)^2$. A first estimate of the trap density was obtained from the standard PR model,[47] where the PR space-charge field is given by

$$E_{sc}^2 = \frac{E_d^2 + E_{og}^2}{(1+B)^2 + B^2(E_{og}/E_d)^2} \qquad (8)$$

where E_d is the diffusion field given by $E_d = K_G k_B T/e = 0.1$ V/μm, $K_G = 3.9$ μm^{-1}, and E_{og} is the projection of $\vec{E}_o$ along $\vec{K}_G$. The solid line in the inset to Figure 10 is a least-squares fit to eq 8, which yields the effective density of photorefractive traps $N_{pr} = K_g^2 \epsilon_r \epsilon_o k_B T/Be^2 = 1.9 \times 10^{15}$ cm^{-3} ($\epsilon_r = 2.9$).

The anisotropy of the diffracted signal with reading beam polarization η_p/η_s in bisA-NPDA:DEH was 6 ± 2, in good agreement with the value predicted from the standard theory of the PR effect. Conclusive evidence for the PR nature of the grating detected by the FWM mixing experiments was provided by 2BC measurements of the grating spatial phase shift, as described in detail in ref 63. The index grating phase ϕ_P as a function of applied field along the grating wave vector is shown in Figure 11 (symbols). At zero field, the phase of the weak index grating formed is near zero degrees (an in-phase grating). Since standard models of the PR effect give a 90° phase shift due to diffusion in zero field, this grating is not photorefractive in nature, but may be due to local processes such as photochromism. Since the electrooptic coefficient of the poled polymer approaches zero as the applied field goes to zero, any PR effect due to charge separation by diffusion that might be present would be extremely difficult to detect. As the field is increased (and hence, r), the phase of the index grating increases until moderate to high fields (25–50 kV/cm), where it plateaus near 90°. This index grating shifted by 90° at high fields is clearly photorefractive in nature, because no moving gratings or frequency shifts were present during grating formation. As the grating was formed, one of the writing beams

increased in intensity as the other writing beam decreased by approximately the same amount (0.6%), giving $\Gamma = 0.33\ cm^{-1}$. This is considerably less than $\alpha = 10\ cm^{-1}$, so net internal two-beam coupling gain was not achieved in this system.

b. NNDN-NAN:DEH. The second cross-linked host NLO polymer, NNDN-NAN (Figure 8b) was composed of the bifunctional monomer *N,N*-(diglycidyl)-4-nitroaniline (NNDN) reacted with the trifunctional nonlinear chromophore *N*-(2-aminophenyl)-4-nitroaniline (NAN). Charge transport was added by doping the polymer with 30 wt % DEH (Figure 9a). A steady-state diffraction efficiency η_{ss} of 10^{-3} was measured by FWM[61] in a 350-μm-thick sample at $E_0 = 8.5\ V/\mu m$ (Table 2). The dynamic behavior of the grating was similar to that of bisA-NPDA:DEH, and η was strongly field dependent. No investigations of the polarization anisotropy or 2BC properties of this material were carried out, so the purported PR origin of the grating should be viewed with caution.

The approach of using an NLO chromophore containing multiple cross-linking sites as a cross-linking agent in a polymer has both advantages and disadvantages. The cross-linking can, in principle, be carried out while the chromophores are aligned in an external electric field, thus locking the alignment of the chromophore into the polymer matrix. This produces a high T_g polymer in which the orientational stability of the chromophores is greatly increased at room temperatures.[18] However, attempts to fully cure bisA-NPDA:DEH (for example) produced a loss of optical quality, perhaps due to phase separation of the polymer and DEH. Even without full curing of the samples, there were sizable inhomogeneities in the optical and electrooptic properties of the material due to uneven cross-linking. Such inhomogeneities in the optical properties may make thermally cross-linked polymers difficult to use for applications.

2. Methyl Methacrylate Copolymer Hosts

Another class of NLO polymers which have been used as hosts for PR materials consist of methyl methacrylate copolymers in which the chromophore is present as a pendant side group. As with the epoxy polymers discussed above, charge (hole) transport is provided by doping the polymer with a small molecule transport agent.

a. A Photoconducting Electrooptic Polymer. The first potential PR material based on a MMA copolymer[19] consisted of a methyl methacrylate backbone with the side-chain chromophore 4′-(dialkylamino)-4-(methylsulfonyl)stilbene. The charge-transporting agent added to this polymer was 1,1-bis[4-(di-*p*-tolylamino)-phenyl]cyclohexane (~4 wt %). An an explicit sensitizing agent, *N,N′*-bis(2,5-di-*tert*-butylphenyl)-3,4:9,10-perylenebis(dicarboximide) (p-dci) was also added to the mixture. Thin films of this material (~1 μm) were corona poled at 100 °C ($E = 170\ V/\mu m$), resulting in an electrooptic coefficient of 2.5 pm/V. Photoconductivity was also demonstrated in this sample at 532 nm. However, no measurements of PR grating formation have been reported for this material.

b. PMMA-PNA:DEH. The first material using a MMA-based copolymer host in which the PR effect was convincingly demonstrated[72] was PMMA-PNA

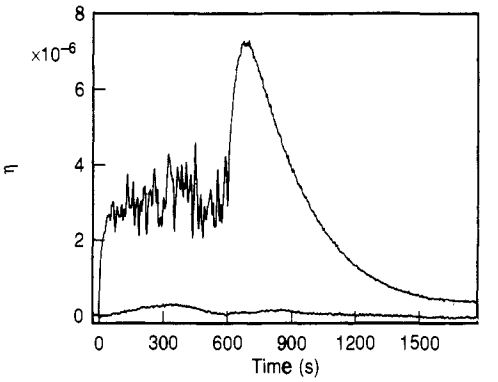

Figure 12. Diffraction efficiency of gratings written in PMMA-PNA:DEH (λ = 647 nm, 1 W/cm^2 writing power, 750-μm beam diameter, and sample thickness 350 μm). Writing time of 600 s with an applied electric field of 11.4 V/μm (upper curve) and without (lower curve). (Reprinted from ref 72. Copyright 1992 Optical Society of America.)

(Figure 8c), which utilizes a methyl methacrylate copolymer host with the nonlinear chromophore *p*-nitroaniline in a pendant side group. The polymer was doped with 30 wt % of the charge-transport agent DEH (Figure 9c) to provide a transport network for photogenerated carriers. The samples in which the PR effect was observed had an absorption coefficient of $\alpha = \sim 1\ cm^{-1}$ at 647 nm (see Table 2).

The grating dynamics observed for PMMA-PNA:DEH are shown in Figure 12. The writing beams are turned on at time $t = 0$. Writing with $E_0 = 11.4\ V/\mu m$ (upper trace), a fast initial rise in the diffraction efficiency η of the reading beam is observed, which slows and saturates after approximately 30 s of writing time. After 30 s, a fast, apparently chaotic oscillation is evident, indicating the competition of two gratings with different characteristic growth times as slight changes occur in the phase of the two writing beams. When the writing beams are blocked at $t = 600$ s, η rapidly increases. Similar grating competition effects have been treated in some detail in the inorganic photorefractive $Bi_{12}SiO_{20}$ by invoking motion of additional carriers, and the increase in η during readout is referred to as revelation.[73] The revealed grating then decays with a time constant much longer than that of grating growth. Writing with zero external electric field (Figure 12, lower trace) produces only a very weak grating which may be due to a weak photochromic effect or to a photorefractive effect occurring in a weak residual field and detected via residual alignment of the chromophores.

The competition and relevation effects may be understood in the following fashion: Two sets of carriers are present, the holes which are generated by the light and drift in the electric field until trapping occurs, and another set of charge carriers which are much less sensitive to the light but are still able to respond to the local electric field. The optical intensity pattern forms a space-charge grating in the holes as usual. The hole space-charge field causes the second set of carriers to move in the opposite direction, forming a second space-charge field which cancels the hole space-charge field. The diffraction efficiency is limited during the writing time because the net electric field from the two sets of carriers is small. When the light is removed, the hole space-charge field decays quickly due to dark conductivity, leaving (revealing) the space-charge field from

the slower second set of carriers, and the diffraction efficiency increases for a time. Eventually, the space-charge field from the second set of carriers also decays. The most likely source of the additional carrier in the PMMA-PNA:DEH system was identified as small ions, possibly coming from the residual solvent in the sample.

Proof of the photorefractive origin of the grating resulted from the measurement of the (index) grating spatial phase by the two-beam coupling and sample translation techniques described previously.[63] The measurements confirmed that the grating produced was predominantly an index, rather than an absorption, grating and that the index grating was shifted 90° from the light intensity pattern.

When λ = 568 nm was used (α = 5.9 cm^{-1}) to create and probe the PR grating, η was increased by a factor of 2 to 3 due to the increased sample absorption and electrooptic coefficient. At the same time, the zero-field photochromic effect discussed above increased in magnitude to between 20 and 30% of the total diffraction efficiency observed at long times with an 11.4 V/μm field across the sample. At short times the signal was still purely photorefractive, as evidenced by measurement of the grating phase, with the rate of the fast initial rise increased at this wavelength.

The grating growth was characterized by assuming an exponential growth of the space-charge field

$$\eta(t) \approx [E_{sc}(1 - e^{-t/\tau})]^2 \quad (9)$$

where E_{sc} is the saturation value of the space-charge field and τ is the characteristic growth time. This behavior is the result of the standard single-charge-carrier model for PR grating formation.[47] The resulting risetime τ of the grating before competition occurs was fit with a power law dependence of the rate ($1/\tau$) on intensity. The power laws were sublinear, with exponents 0.76 ± 0.09 and 0.62 ± 0.12 for 568 nm (two samples) and 0.55 ± 0.25 for 647 nm. Sublinear rates have been discussed extensively[74] for inorganic crystalline photorefractives such as $BaTiO_3$. Recent more detailed measurements in $BaTiO_3$ showed that the speeds have a complex intensity dependence which appear to be sublinear over a small range.[75] The more complex dynamics were explained by a combination of shallow and deep traps for carriers;[76] similar physical processes may be present in PMMA-PNA:DEH.

In bisA-NPDA:DEH,[17] the time scale of the growth of the grating at 1 W/cm^2 was 1 to several minutes. At the same power level, the growth time in PMMA-PNA:DEH was approximately 1 s, an increase in rate of 2 orders of magnitude, even though both materials had approximately the same absorption coefficient. This was attributed to an increase in the quantum efficiency of charge generation in PMMA-PNA:DEH, due to the formation of a charge-transfer complex between the PNA and DEH.

c. PMMA-MSAB:TTA:BDK. Another MMA-based copolymer in which photorefractivity has been reported[77] is a copolymer of methyl methacrylate (MMA) and 4′-[(6-(methacroyloxy)hexyl]methylamino]-4-(methylsulfonyl)azobenzene (Figure 8d). This polymer is designated polymer III in ref 78 and will be referred to as PMMA-MSAB for notational consistency. The charge transport agent for this material was 31 wt % of tri-*p*-tolylamine (TTA; Figure 9d), and the charge

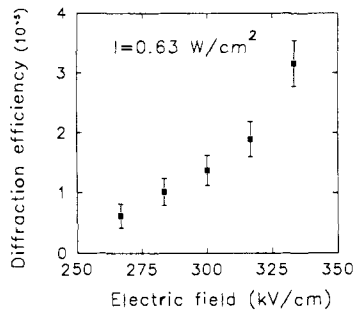

Figure 13. Electric field dependence of the diffraction efficiency in PMMA-MSAB:TTA:BDK. (Reprinted from ref 77. Copyright 1992 American Institute of Physics.)

generator was 0.03 wt % boron diketonate (BDK; Figure 9e). This polymer has the advantage of using a more nonlinear chromophore than PMMA-PNA and contains an explicit charge generating agent. (A systematic study of the effect of a charge-generating agent on the PR properties of PMMA-PNA:DEH is presented in section III.A.3.)

The necessary prerequisites for the PR effect were demonstrated on a thin, high-temperature-poled (70 °C, 27 V/μm) polymer film (11-μm thickness). A stable electrooptic coefficient of 1.3 pm/V and nonzero photoconductivity were measured. The quantum efficiency of charge generation was measured and found to obey the Onsager model (cf. section II.C.2), with a maximum value of 1.14% at an applied field of 136 V/μm.

Field-dependent gratings were observed in a 100-μm-thick sample of this material as shown in Figure 13 and interpreted as photorefractive.[77] A peak diffraction efficiency of 3×10^{-5} was measured. This thick sample was also high-temperature poled (70 °C, 10 V/μm), but no measurements of the value or stability of the electrooptic coefficient were reported. Although the gratings appeared to be reversible, no measurement of the polarization anisotropy was presented. More significantly, no measurements of asymmetric beam coupling or the PR phase shift were reported. Therefore the purported photorefractive origin of the grating should be viewed with caution.

3. Sensitization with Fullerenes and Other Photocharge Generators

As discussed above, addition of a dopant to improve the generation of charge is expected to improve the PR properties of a material. A systematic study[79,80] of the effect of sensitizing agent has been carried out in PMMA-PNA:DEH. The optical absorption of this material at 647 nm was low enough to allow the effect of different sensitizers to be easily studied.

The sensitizers which were incorporated into the polymer were 2,4,7-trinitro-9-fluorenone (TNF; Figure 9f), a solubilized squaryllium dye (Figure 9g), the charge-transfer complex anthracene-tetracyanoquinodimethane (anthracene-TCNQ), C_{60}, and *N,N*′-bis(2,5-di-*tert*-butylphenyl)-3,4:9,10-perylenebis(dicarboximide) (p-dci; Figure 9h). The photorefractive properties of 350-μm-thick samples were measured by FWM in the geometry discussed in the previous section (see Table 2). The results are shown in Figure 14, with an applied field of E_0 = 11.4 V/μm. The steady-state diffraction efficiencies and approximate grating growth rates have been characterized[79,80] and it was found that C_{60} and

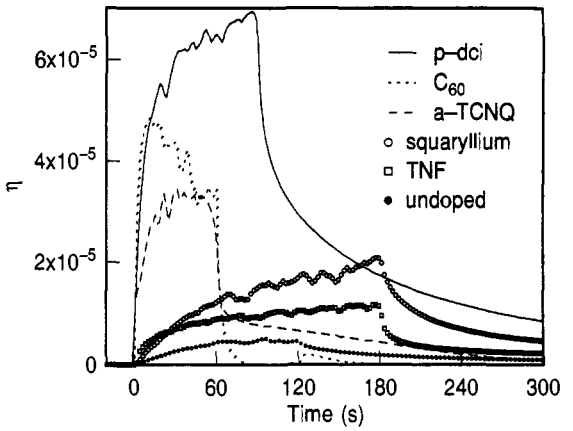

Figure 14. Diffraction efficiency shown as a function of time for PMMA-PNA:DEH with various charge generating agents. All samples are 350-μm thick, E_0 = 11.4 V/μm, λ = 647 nm, writing intensity = 1 W/cm^2, and the generator concentrations are given in Table 2. For all data scans, the writing beams are turned on at t = 0 and the gratings are written to saturation. Although the sample containing p-dci has the largest η_{ss}, the signal is also accompanied by a strong photochromic response, making C_{60} the best choice of generating agent of those shown.

p-dci provide the largest enhancement of η_{ss} and τ^{-1}, while causing only a small increase in the optical absorption. Additionally, the magnitude of competing (photochromic) absorption gratings due to the photoreduced donor or to other photochemical processes can be estimated from FWM measurements with no applied field and was found to be ~5% for p-dci but <1% for C_{60}. C_{60} is therefore the best choice of these agents for sensitizing PMMA-PNA:DEH. C_{70} was also tested and was found to have sensitizing capabilities similar to C_{60} as well as greater absorption in the near infrared, which may be useful in potential applications of polymeric PR materials at longer wavelengths.

The properties of the specific combination PMMA-PNA:DEH:C_{60} were investigated in more detail.[79] Addition of C_{60} increases the absorption of the material in the red and near-infrared region of the spectrum, as discussed in section II.C.1 (see Figure 3). Gratings written in samples doped with C_{60} show the same qualitative behavior as those written in undoped samples, described in section III.B.2.b. In particular, asymmetric two-beam coupling was observed, with a gain coefficient of Γ = 0.6 cm^{-1} for a sample with 0.1 wt % C_{60} at a field of E = 11.4 V/μm.

The observed steady-state diffraction efficiency η_{ss} and the initial rate of grating growth τ^{-1} obtained by early-time fits to eq 9 are shown as functions of C_{60} concentration in Figure 15, parts a and b, respectively. The value of η_{ss} increases rapidly at low C_{60} concentrations, but reaches a plateau above 0.02 wt % C_{60}. The grating growth rate increases over the whole concentration range, increasing the most rapidly at highest concentrations. This improvement in the values of η_{ss} and τ^{-1} cannot be achieved in the undoped sample by writing the grating with a shorter wavelength where the sample absorption is higher.

In separate measurements of the grating growth rate as a function of the writing intensity, a sublinear power law was observed with an exponent of 0.35, a value considerably lower than those found for the undoped samples (0.55 to 0.76).[72] This suggests that addition of C_{60} increases the shallow trap concentration.[75]

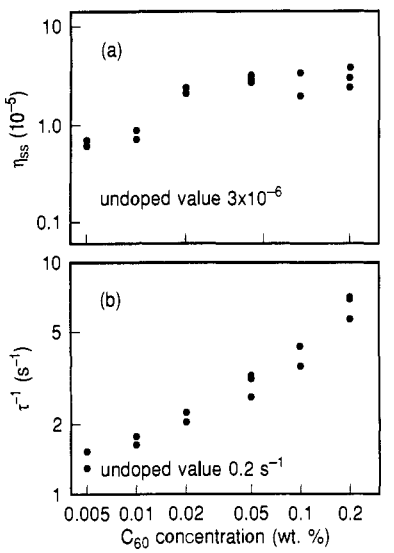

Figure 15. η_{ss} and τ^{-1} as a function of C_{60} concentration (log–log scale) in PMMA-PNA:DEH:C_{60}, for I = 1 W/cm^2 and E = 11.4 V/μm. The values for the undoped sample are given in the figures. (Reprinted from ref 79. Copyright 1992 Optical Society of America.)

Roughly a factor of 2 increase in quantum efficiency was measured in this material upon doping. The authors concluded that most of the reason for the increased growth rate upon doping (Figure 15b) is due to the increased absorption and therefore higher concentration of carriers available to form a space charge field. The increase in η_{ss} (Figure 15a) could be due to an increased shallow trap density and a change in the balance between trapping and detrapping caused by the increased carrier generation.

4. Linear Epoxy Hosts

a. bisA-NAT:DEH, Permanently Poled. The third type of NLO polymer that has served as the host for a PR polymer mixture is a linear epoxy in which the NLO chromophore is present as a pendant side group. One such linear epoxy is bisA-NAT[81] (Figure 8e), which is formed by the reaction of bisphenol A diglycidyl diether (bisA) with the nonlinear chromophore nitroaminotolan (NAT). Although chemically related to the cross-linked nonlinear epoxy materials discussed above, NAT has only two reactive sites and the result of the reaction is a linear polymer. To form the PR polymer, bisA-NAT was doped with the charge transporting molecule DEH (Figure 9a; Table 2). The chromophore acts as a charge generator and the polymer furnishes the necessary charge traps.

In the first study of this material,[80] in contrast to other PR polymer samples described above, the bisA-NAT:DEH mixture had a sufficiently high T_g (>90 °C) that the chromophores could not be efficiently aligned at room temperature. Therefore this sample was high temperature poled as usual by heating the sample to 90 °C, slightly below T_g, and applying an electric field of 55 V/μm across the material. The resulting permanently poled nonlinear polymer had a nonlinear optical coefficient of n^3r_e = 3.4 pm/V at E_0 = 0 V/μm, which was stable for at least several months. In addition, n^3r_e was observed to have a linear dependence on the applied field, with a slope of 0.027 (pm/V)/(V/μm) due to quadratic effects.

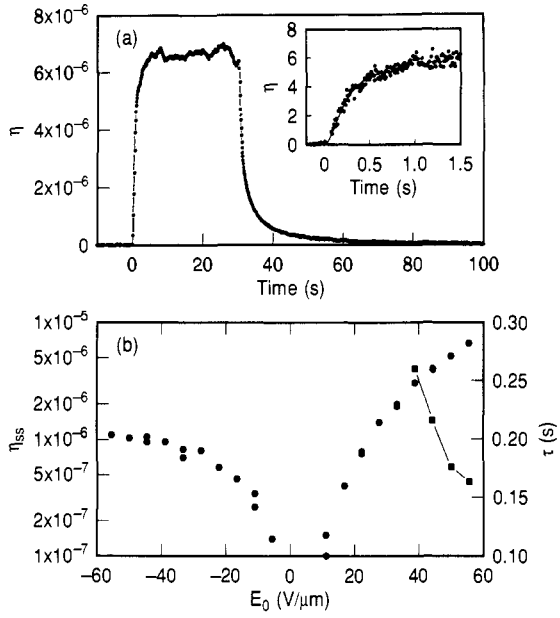

Figure 16. (a) η shown as a function of time for a permanently poled sample of bisA-NAT:DEH (λ = 647 nm, E_0 = 55 V/μm, writing intensity = 1 W/cm^2, sample thickness = 36 μm). The writing beams are turned on at t = 0 and the grating grows to saturation in less than 2 s. The diffraction efficiency remains constant until the writing beams are turned off at t = 30 s, and decays quickly in the presence of the reading beam only. The inset shows the grating growth along with a fit to eq 9, with τ = 160 ms. Part b shows FWM steady-state diffraction efficiencies η_{ss} (left ordinate, circles) versus E_0 for a 36-μm sample of bisA-NAT:DEH at λ = 647 nm. FWM grating growth times are also shown for the highest applied fields, where they could be accurately measured (right ordinate, squares). (Reprinted from ref 80. Copyright 1993 Society of Photo-Optical Instrument Engineers.)

The diffraction efficiency is shown as a function of time for bisA-NAT:DEH in Figure 16a (E_0 = 55 V/μm, sample thickness of 36 μm). The writing beams are turned on at t = 0 and both writing beams are blocked at t = 30 s. The signal shows a rapid initial rise, which saturates after approximately 2 s at η_{ss} = 6.6 × 10^{-6}, and remains constant thereafter. When the writing beams are blocked, the signal shows a rapid, nonexponential decay. The rapid initial rise in η is shown in the inset of Figure 16a and is analyzed in the usual fashion (eq 9). The fit is shown in the inset, with τ = 160 ms.

The field dependence of η_{ss} is shown in Figure 16b (circles, left ordinate). For E_0 = 0, η is below the detection limit of 10^{-8}, confirming that even though the material has a finite electrooptic coefficient, the PR effect is not observed. This is a result of the absence of photoinduced charge generation and the absence of drift-assisted charge transport. The steady-state diffraction efficiency η_{ss} reaches a maximum value of 8 × 10^{-6} at E_0 = 55 V/μm. The asymmetry between η_{ss} observed for positive and negative E_0 is due to the lower effective value of n^3r_e at applied fields which oppose the original poling field. The measured polarization anisotropy was 9.5 ± 1, in good agreement with theory. The dependence of τ on E_0 is shown in Figure 16b (squares, right ordinate) at the highest fields, where it could be accurately determined. τ decreases with increasing field, due presumably to the increasing efficiency of charge generation.

As for bisA-NPDA:DEH, the measured field dependence of η_{ss} and n^3r_e allowed a rough determination of the effective density of photorefractive traps N_{pr} = 2.8 × 10^{16} cm^{-3} (ϵ_r = 3). This trap density is more than 1 order of magnitude larger than for bisA-NPDA:DEH.[17]

The 2BC gain for bisA-NAT:DEH was measured at 647, 676, and 753 nm. At all wavelengths, the observed increase in one beam was always accompanied by an approximately equal decrease in the other beam, indicating an index grating with a nonzero phase shift between the intensity pattern and the index modulation. This nonzero phase shift, which was estimated to be near 90° by a grating translation technique,[63] is proof of the photorefractive origin of the index modulation. The gain coefficient Γ and absorption coefficient α are given as a function of wavelength in Table 2.

Net gain, i.e., $\Gamma - \alpha > 0$, was not observed in this material at these wavelengths. Further red-shifting of the optical wavelength is not practical due to increasing response time of the material (20 s at 753 nm), which is due to lower total charge generation accompanying the lower absorption. One possible route to increasing the gain is to increase the nonlinearity by refining the poling process. Much higher electrooptic coefficients ($r_{13} \approx$ 8 pm/V) have been achieved in a thin film (1.6 μm) of bisA-NAT with no DEH added.[81] Another route is through modification of the chromophore, substitution of the $-NO_2$ acceptor group with $-SO_2CF_3$, for example, which shifts the absorption peak of the chromophore to the blue[82] and inclusion of a separate and more efficient charge generating agent to increase the number of charges generated while decreasing the amount of total absorption at the operating wavelength.

b. BisA-NAT:DEH, Aligned at Room Temperature. In a separate study[83] of the bisA-NAT:DEH system, the bisA-NAT host polymer had a lower T_g of about 59 °C as a result of reduced reaction time. This along with the additional plasticization of the polymer due to 40 wt % doping with DEH (see Table 2) allowed alignment of the material at room temperature. The photoconductivity per unit light intensity at 650 nm was measured to be (8.7–10) × 10^{-11}(Ω–cm)$^{-1}$ per W/cm^2, which decayed with illumination over some minutes by roughly a factor of 2. As in the other room-temperature-poled materials, the electrooptic response was linear in the applied field. By using 145-μm-thick films and an optical wavelength of 650 nm where the optical absorption coefficient was 118 cm^{-1}, gratings with a diffraction efficiency of 1.1 × 10^{-3} were observed with an applied field of 13.8 V/μm. No gratings were observed in zero bias field, and no beam-coupling measurements were reported.

Similar to the earlier work on BSO[73] and on PMMA-PNA:DEH[72] described in section III.A.2.b, grating competition and revelation were observed. An interpretation was proposed[83] on the basis of two types of traps denoted A and B. The A traps are photosensitive, while the B traps have low photogeneration efficiencies and trap charge liberated from the type A traps. Grating formation involves movement of charge from the type A traps to the type B traps, which produces a peak in the diffraction efficiency followed by a reduction as the space-charge field first increases, then decreases as the type B traps remove the charge liberated by the type A traps. After a dark period, if

Table 3. Optical Properties of Doped Materials Based on Charge-Transporting Polymer Hosts

polymer	chromophore[a]	sensitizer[b]	λ (nm)	α (cm^{-1})	η_{ss}[c]	τ (s)[d]	Γ (cm^{-1})[c]
PVK[86]	DEANST	C_{60}[e]	633	205	2×10^{-5} [f]		
PVK[20,80]	FDEANST	TNF	647	32	8.5×10^{-3} [g]	0.075	11.0[g]
			676	17	1.3×10^{-2} [g]	0.135	9.9[g]
			753	1.4	1.0×10^{-3} [g]	7.6	8.6[g]
PVK[89]	PDCST	TNF	753	2.3	3.7×10^{-3}		7.8
PVK[89]	MBANP	TNF	753	0.9	1.7×10^{-4}		2.6
PVK[89]	MTFNS	TNF	753	0.6	1.2×10^{-5}		1.2
PVK[89]	DEAMNST	TNF	753	10	1.5×10^{-3}		8.0
PVK[89]	DEANST	TNF	753	10	2.3×10^{-3}		5.0
PVK[89]	DEACST	TNF	753	11	2.0×10^{-4}		2.1
PVK[89]	DEABNB	TNF	753	40	9.9×10^{-5}		3.2
PVK[89]	DTNBI	TNF	753	49	3.8×10^{-4}		5.4
PVK[89]	FDEANST	p-dci[h]	753	<0.5	4.5×10^{-4}	23	2.3
PVK[89]	FDEANST	C_{60}[h]	753	0.9	1.1×10^{-3}	3.0	9.0
PBPES[43]	coumarin-153[i]	C_{60}[h]	647	14	7.7×10^{-6} [j]	0.09	0.25[j]
PBPES[43]	coumarin-153[i]	TNF	647	7.4	5.2×10^{-6} [k]		0.27[k]
PBPES[43]	FDEAMNST[l]	C_{60}[h]	753	1	1.1×10^{-4} [m]	0.04	1.7[m]

[a] Chromophore concentration 33 wt %, unless otherwise noted. The structures and names are given in Figure 18. [b] Sensitizer concentration 1.3 wt %, unless otherwise noted. The structures and names are given in Figure 9. [c] Sample length 125 μm, E = 32 V/μm, unless otherwise noted. [d] Intensity 1 W/cm^2, unless otherwise noted. [e] 1.9 wt %. [f] Sample length 100 μm, E = 50 V/μm. [g] E = 40 V/μm. [h] 0.2 wt %. [i] 20 wt %. [j] Sample length 350 μm, E = 11.4 V/μm. [k] Sample length 350 μm, E = 14.3 V/μm. [l] 40 wt %. [m] Sample length 175 μm, E = 16 V/μm.

(a) PVK (b) PBPES

Figure 17. Charge-transporting polymers which have been used as hosts for photorefractive polymers: (a) poly(*N*-vinylcarbazole) (PVK) and (b) poly[(4-*n*-butoxyphenyl)-ethylsilane] (PBPES).

the uniform reference beam is turned on, the type B grating is revealed and then decays. The dark decay time of the type B grating of some minutes was increased slightly in the presence of a large dc electric field. This model was interpreted as being consistent with the observed fatigue of the photoconductivity, although it was unable to explain why optical illumination was required to reveal the type B grating.

B. Doped Materials Based on Charge-Transporting Polymers

Unlike the case for nonlinear polymers discussed above, the number of polymers which are inherent charge transporters is quite small. To date, only two charge-transporting polymers have been used as hosts for photorefractive polymer mixtures. The first and much more thoroughly investigated of these polymers is poly(*N*-vinylcarbazole) (PVK), and the second is a poly(silane) derivative. All of the charge-transporting polymer–NLO chromophore–sensitizer combinations which have been reported as photorefractive are listed in Table 3, with the reported values for their photorefractive parameters. The structures of the polymers are given in Figure 17, and the structures of the NLO chromophores are given in Figure 18. Other charge-transporting polymers that should be considered as hosts are poly(*p*-phenylenevinylene), poly(thienylenevinylene), and similar materials[84,85] which show photoconductive properties yet have a region of optical transparency.

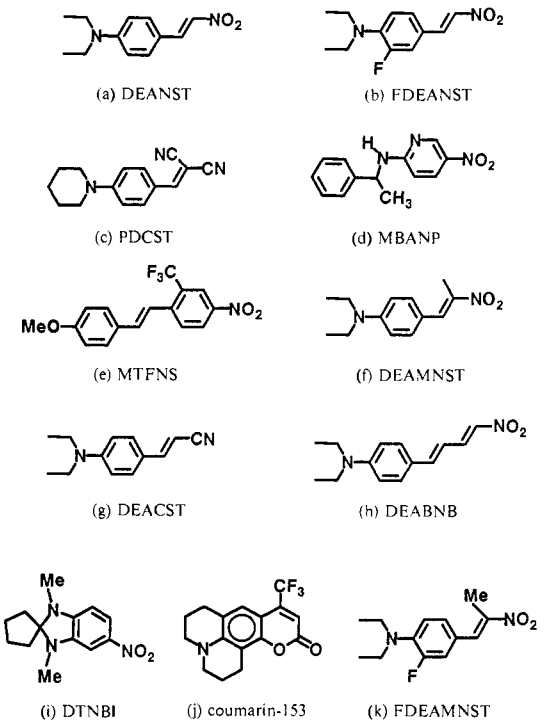

Figure 18. Nonlinear optical molecules which have been added to charge-transporting polymers: (a) 4-(diethylamino)-(*E*)-β-nitrostyrene (DEANST); (b) 3-fluoro-4-(diethylamino)-(*E*)-β-nitrostyrene (FDEANST); (c) (4-piperidinobenzylidene)-malononitrile (PDCST); (d) (+)-2-[(α-methylbenzyl)amino]-5-nitropyridine (MBANP); (e) 4-methoxy-2′-(trifluoro methyl)-4′-nitrostilbene (MTFNS); (f) 4-(diethylamino)-(*Z*)-β-methyl-(E)-β-nitrostyrene (DEANMST); (g) 4-(diethylamino)-(*E*)-cinnamonitrile (DEACST); (h) (*E*,*E*)-1-[4-(diethylamino)-phenyl]-4-nitrobutadiene (DEABNB); (i) 1,3-dimethyl-2,2-tetramethylene-5-nitrobenzimidazoline (DTNBI); (j) coumarin-153 (C-153); and (k) (*E*)-β-nitro-(*Z*)-β-methyl-3-fluoro-4-(diethylamino)styrene (FDEAMNST).

1. PVK-Based Systems

a. PVK:DEANST:C_{60}. The first reported[86] PR polymer based on PVK (Figure 17a) consisted of PVK doped with the NLO chromophore 4-(diethylamino)-(*E*)-β-nitrostyrene (DEANST, 32 wt %; Figure 18a) and the fullerene C_{60} (1.9 wt %) as a charge generating

agent. The PR properties were examined by FWM experiments at λ = 633 nm in 100-μm-thick poled samples (poled at 70 °C with E = 25 V/μm; see Table 3). A field-dependent diffraction efficiency was observed, which peaked at $\eta = 2 \times 10^{-5}$ at E = 50 V/μm. This experiment was performed using a grating spacing of 5 μm and with the reading beam s-polarized. The absorption coefficient at 633 nm in this composition was quite large; using the reported optical density of 0.89 in a (presumed) 100-μm thickness gives an optical absorption coefficient of 205 cm^{-1}. In the initial report of this material the field-dependent gratings were taken as proof of the PR effect. In recent additional work,[87] 2BC measurements have been reported showing asymmetric beam coupling and actually establishing the PR nature of the gratings.

b. PVK:FDEANST:TNF. A second PVK-based system reported in the literature consists of PVK (Figure 17a) doped with the NLO chromophore 3-fluoro-4-(diethylamino)-β-nitrostyrene (FDEANST, 33 wt %; Figure 18b), with 1.3 wt % of 2,4,7-trinitro-9-fluorenone (TNF; Figure 9f) added as a long wavelength photosensitizer.[20] FDEANST has reduced absorption in the red relative to the unfluorinated analog DEANST, and therefore should eliminate absorption by the chromophore in the red and infrared region of the spectrum where the well-known PVK:TNF charge-transfer complex[30,88] absorbs. The glass-transition temperature T_g of the 125-μm-thick films was approximately 40 °C. Therefore these films could be poled at room temperature by the application of an electric field, and depoling occurred automatically when the E field was removed.

The field dependence of the gratings of PVK:FDEANST:TNF was examined in p-polarized FWM experiments. For λ = 647 and 676 nm the grating growth times are comparable to the fastest NLO-polymer-based PR polymers,[72,79] and η saturates after approximately 1 s. For λ = 753 nm where the optical density of the material and the power density in the write beams are smaller, it takes 20 to 30 times longer for the diffraction efficiency to reach saturation. In the absence of an externally applied electric field, η is below the detection limit of 10^{-8} at 753 and 676 nm. At 647 nm, a weak grating is observed to grow on the time scale of several minutes in zero field. 2BC measurements reveal this grating to be a 0° phase-shifted index grating.[63] This grating may be due to photochromic processes initiated by absorption by the NLO chromophore, which accounts for approximately 10% of the total absorption at 647 nm but is negligible at the longer wavelengths.

As the applied field increases, the steady-state diffraction efficiency η_{ss} increases proportional to $E_0^{(3.6\pm0.3)}$ due to the increase in $n^3 r_e$ and in the space-charge field. This is shown in Figure 19. At λ = 647 nm, η_{ss} reaches a value of 1.2% at E_0 = 40 V/μm. This value of η_{ss} is 1–2 orders of magnitude larger than the highest diffraction efficiency reported previously for a photorefractive polymer,[61,83] if equal sample lengths are assumed. At 676 nm, η_{ss} is also on the order of 1%, but η_{ss} is an order of magnitude smaller at 753 nm. This peak diffraction efficiency is 3 orders of magnitude larger than that of the first reported PVK-based system,[86] at comparable sample thicknesses and fields.

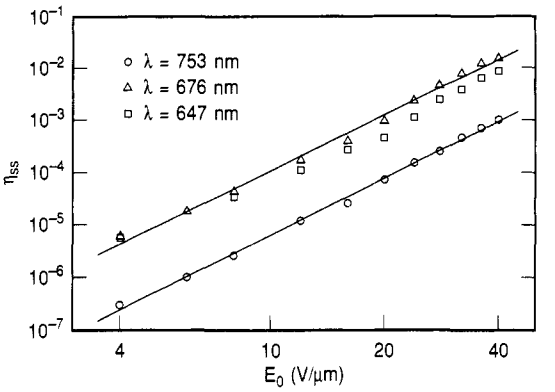

Figure 19. η_{ss} versus E_0 for PVK:FDEANST:TNF at the wavelengths indicated. Solid lines are power-law fits to the 676- and 753-nm data, with exponents 3.5 and 3.6, respectively. (Reprinted from ref 20. Copyright 1993 Optical Society of America.)

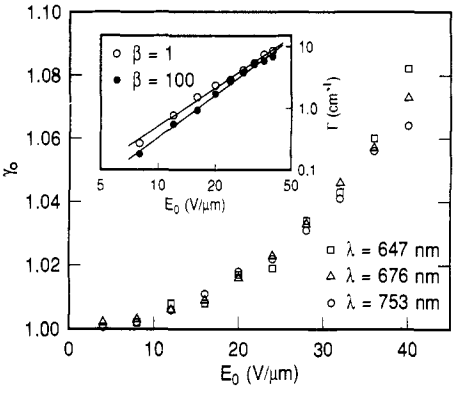

Figure 20. γ_0 versus E_0 for PVK:FDEANST:TNF at the wavelengths indicated and β = 1. The inset shows Γ vs E_0 for 753 nm and the β values indicated. α = 1.4 cm^{-1} at 753 nm. (Reprinted from ref 20. Copyright 1993 Optical Society of America.)

Two-beam coupling experiments verified that the field-dependent gratings observed in the FWM experiments were photorefractive in origin. The beam-coupling ratio γ_0 for PVK:FDEANST:TNF is shown in Figure 20 as a function of E_0 at a beam power ratio β = 1 for 647, 676, and 753 nm. The normalized beam-coupling gain coefficient Γ given by eq 7 is shown in the inset of Figure 20, for λ = 753 nm, both for β = 1 and for β = 100. It was experimentally verified that Γ is essentially independent of β over the range 1 to 10^4 for the PVK:FDEANST:TNF system. For λ = 753 nm with a field of 40 V/μm across the sample, Γ reached a value of 8.6 cm^{-1}, which exceeded the material's absorption coefficient α of 1.4 cm^{-1} by more than a factor of 6. This makes PVK:FDEANST:TNF the first organic photorefractive material for which net internal gain has been observed.[20] Although Γ was somewhat larger for λ = 647 nm (11.0 cm^{-1}) and 676 nm (9.9 cm^{-1}), the absorbance of the material at these wavelengths was greater, 32 and 17 cm^{-1}, respectively, and net gain was not observed. Since the material is poled by the applied E field during the beam-coupling measurement, the sign of the electrooptic coefficient, and therefore the direction of beam coupling is controlled by the direction of the field. If the field direction is reversed, the beam showing gain is switched from one write beam to the other, which may be useful in some applications.

The photorefractive performance of PVK:FDEANST:TNF is significantly better than that of all previously described organic photorefractive materials for several reasons. PVK:FDEANST:TNF is the first organic material to show an internal two-beam coupling gain coefficient Γ that exceeds the absorption coefficient. Its maximum diffraction efficiency of 1% is 1–2 orders of magnitude larger than values reported for other PR polymers. The grating growth time of about 100 ms is comparable to that of the fastest known photorefractive polymer. These results make PVK:FDEANST:TNF comparable to some of the well-known inorganic crystals (see section V).

c. Other PVK:chromophore:sensitizer materials. The generality of the photorefractive properties of PVK:FDEANST:TNF have been investigated[89] by constructing other PVK-based polymers by varying both the chromophore and sensitizer. The nine NLO chromophores which have been combined with PVK:TNF to produce a photorefractive polymer are listed in Table 3, and their structures are given in Figure 18, parts a–i. The optical absorption coefficient α at 753 nm for each PR polymer sample is shown in Table 3. The nine nonlinear chromophores have a variety of chemical structures and were selected in order to begin to evaluate various tradeoffs in nonlinearity, transparency and size. In two of these chromophores (MBANP, DTNBI) a single aromatic ring constitutes the π-conjugated system. Five of the compounds (FDEANST, PDCS, DEAMNST, DEANST, DEACST) have a styrene π-conjugated structure while the remaining two (MTFNS, DEABNB) possess what may be considered to be an extended (stilbene and phenylbutadiene, respectively) styrene π-conjugated system. The optimization of the so-called "efficiency–transparency" tradeoff in these systems, which is a requirement for obtaining net gain, is similar to the same issue encountered in application of organic chromophores to frequency doubling.[44]

The PR response of these materials was characterized by both FWM and 2BC at 753 nm. The PR samples were 125 μm thick, and the bias field was $E_0 = 32\ V/\mu m$. As described previously,[20,80] the samples were poled at room temperature. Table 3 shows results of the PR measurements of η_{ss} (column 6) and Γ (column 8) for samples containing each of the nine chromophores. All samples exhibited asymmetric two-beam coupling, proving the PR nature of the gratings observed. Quantitatively, these samples exhibited a wide variation in their PR properties. Over the range of chromophores added to the polymer, η_{ss} varies by more than 100, with the largest values occurring in the samples doped with the styrene-based chromophores and the smallest values occurring in samples containing the larger chromophores MTFNS and DEABNB. Γ varies by more than 6 over the range of materials and the ordering of the Γ values among the materials generally reflects the ordering of the values of η_{ss}. Net internal gain ($\Gamma - \alpha > 0$) is achieved in samples containing the second through the fifth chromophore listed in Table 3. It is apparent that the failure to achieve net gain in samples containing the remaining five chromophores is due to higher optical absorption and not lower 2BC gain.

The three sensitizers which have been combined with PVK:FDEANST are also listed in Table 3, along with the PR properties η_{ss} (column 6), Γ (column 8), and the $1/e$ risetime τ of the space charge field (column 7). Varying the sensitizer changes the rate at which the mobile charges are generated in the material by varying both the total absorption due to the sensitizer (column 5) and the quantum efficiency of charge generation ϕ (not explicitly measured for each system). The utility of different sensitizers is reflected in the growth time τ, which has the smallest value (fastest grating growth) for the sample containing C_{60} and the largest value for the sample containing p-dci. PVK:FDEANST with no explicit sensitizer has no observable diffraction efficiency or beam coupling gain at 753 nm. It is apparent that varying the sensitizer also influences both η_{ss} and Γ. C_{60} provides the largest PR response of the three sensitizers for PVK:FDEANST, which agrees with previous sensitization studies of the PR polymer PMMA-PNA:DEH.[79,80] It is likely that in addition to providing increased generation of charges, C_{60} acts to increase the density of traps[79] in the material. Direct measurements of ϕ would be helpful in understanding in more detail the usefulness of various sensitizers.

The PR performance of these materials as a function of the structure of the NLO chromophore is influenced by many factors, most notably the electrooptic coefficient. The electrooptic coefficient achieved at a given field reflects the hyperpolarizability (β) of the molecule, the ground-state dipole moment, and the degree to which the chromophore plasticizes the polymer. The orientational enhancement effect (see also section IV.C), which has been proposed to occur in the parent material PVK:FDEANST:TNF, should also occur in these samples, and is also a sensitive function of the orientational response of the chromophores. These factors make the detailed behavior of the PR properties of the materials a complicated function of the chromophore structure. One apparent trend is that the PR response of the material decreases as the size of the chromophore increases. This is most likely due to the increasingly hindered orientational response of the larger chromophores, which reduces both the degree of poling due to the external field (and therefore r_e) and the enhancement due to the internal space charge field. Previous studies of molecular hyperpolarizabilities have shown that β generally increases as the conjugation length between the donor and acceptor ends of the chromophore increases,[90] and the ability of the molecule to orient generally decreases with increasing molecular size and deviation from a spherical shape, particularly well below T_g.[91,92] This suggests the importance of maximizing the orientational response of the molecule to an electric field, particularly as the PR grating is being written, even at the expense of decreasing the inherent nonlinearity of the molecule.

2. Poly(silane)-Based Systems

A second charge-transporting host polymer that has been investigated[43] is poly[(4-*n*-butoxyphenyl)ethylsilane] (PBPES; Figure 17b). To achieve optical nonlinearity in the resulting PR mixture, either coumarin-153 (C-153; Figure 18j) or (*E*)-β-nitro-(*Z*)-β-methyl-3-fluoro-4-(*N*,*N*-diethylamino)styrene (FDEAMNST; Figure 18k) was added to the polymer as a dopant. In addition to the NLO chromophore, a small

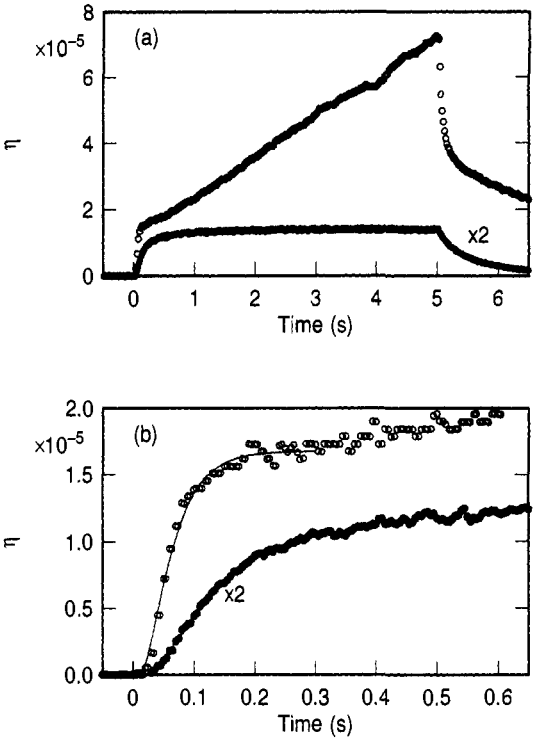

Figure 21. Time dependence of η at E_0 = 11.4 V/μm, λ = 647 nm, and 1 W/cm^2 writing intensity for PBPES:C-153:C_{60} (filled circles), and PBPES:FDEAMNST:C_{60} (open circles). (a) Writing beams are turned on at t = 0 and turned off at t = 5 s. For both materials η exhibits a fast initial rise, which saturates for PBPES:C-153:C_{60} in < 0.5 s but continues to increase at a slower rate for PBPES:FDEAMNST:C_{60}. Part b shows the expansion of the initial rise for both materials and fits to eq 9, with τ = 86 ms for PBPES:C-153:C_{60} and τ = 39 ms for PBPES:FDEAMNST:C_{60}. (Reprinted from ref 43. Copyright 1993 Optical Society of America.)

amount of either 2,4,7-trinitro-9-fluorenone (TNF; Figure 9f) or the fullerene C_{60} was included to photogenerate holes at the experimental wavelengths 647 and 753 nm, a spectral region in which the poly(silane) and NLO chromophore are transparent.

Three specific PBPES:chromophore:sensitizer combinations were investigated[43] (see Table 3): PBPES:C-153:C_{60}, PBPES:C-153:TNF, and PBPES:FDEAMNST:C_{60}. As before, the combination of low intrinsic glass transition temperature of PBPES ($T_g \sim 55$ °C), the plasticization of the PBPES by the NLO chromophore, and the presence of some amount of residual solvent allowed alignment of the NLO chromophores at room temperature. Figure 21 shows the diffraction efficiency of the grating measured by FWM as a function of time for PBPES:C-153:C_{60} (filled circles) and PBPES:FDEAMNST:C_{60} (open circles). Figure 21a shows a scan in which both of the writing beams are turned on at time t = 0 and turned off after a 5-s write. For both samples, η shows a rapid initial rise, which fully saturates in less than 1 s for PBPES:C-153:C_{60}. For PBPES:FDEAMNST:C_{60}, the fast initial rise is followed by a much slower rise which saturates after ~30 s (not shown). The rapid rise of η in PBPES:FDEAMNST:C_{60} was attributed to the growth of E_{sc} and the slower rise to either a second set of traps or to the orientational response of the chromophore to E_{sc}, which may act to enhance the diffraction efficiency (see section IV.C). The τ values were 39 and 86 ms, for PBPES:FDEAMNST:C_{60} and PBPES:C-153:C_{60}, respectively. The former value is the fastest reported rise time for a PR polymer to date.

The steady-state diffraction efficiency η_{ss} was observed to grow approximately at $E_0^{2.8}$ over the full range of applied field in the samples in which C-153 is the chromophore, and for E_0 < 4 V/μm in PBPES:FDEAMNST:C_{60}. For E_0 > 8 V/μm, η_{ss} appeared to follow a field dependence of $\sim E_0^{2.0}$. The cross-over behavior in the field dependence of PBPES:FDEAMNST:C_{60} suggested a saturation of the space-charge field at ~8 V/μm, an effect not observed in the related polymer PVK:FDEANST:TNF,[80] possibly due to a much lower concentration of traps are available to hold the generated charges in PBPES than in PVK.

The photorefractive origin of the field-dependent gratings was conclusively proven by the observation of asymmetric 2BC for all three cases.[43] For PBPES:C-153:TNF (E_0 = 14.3 V/μm, λ = 647 nm) the gain coefficient Γ was 0.27 cm^{-1}. For PBPES:C-153:C_{60} with E_0 = 11.4 V/μm, the gain coefficient was observed to be Γ = 0.25 cm^{-1}. As expected from its larger diffraction efficiency, larger 2BC gain was observed in PBPES:FDEAMNST:C_{60}. The temporal behavior of the 2BC gain contains both the fast and slow features seen in the diffraction efficiency. For E_0 = 11.4 V/μm, a gain coefficient of Γ = 1.7 cm^{-1} was observed at 753 nm after ≃20 s at 1 W/cm^2. The absorption coefficient was α ≈ 1 cm^{-1} at 753 nm, giving a net gain coefficient of $\Gamma - \alpha$ = 0.7 cm^{-1}. This is the second class of polymeric photorefractive material (PVK-based materials constitute the first class[20]) in which net internal gain has been observed.

C. Fully Functionalized (Single Component) Polymers

The last class of polymers that have been considered in the literature as candidate PR materials are composed of fully functionalized polymers. Polymers which have both the NLO chromophore and the charge-transporting molecule attached to the polymer backbone could in principle have several advantages over those in which any (or all) of these components is present as a guest molecule. The first potential advantage is the stability of such single component systems against phase separation and sublimation during sample preparation. The second is stability of the electrooptic coefficient. Guest–host polymer systems are generally observed to have lower glass transition temperatures than single component systems and, therefore, are less orientationally stable after being high temperature poled. This advantage becomes less important (and potentially even a disadvantage) when the role of the orientational enhancement mechanism is understood (section IV.C).

There also exist several potential disadvantages of this approach. The first is the possibility of interrupting conduction pathways in such systems. In conducting polymers charge transport occurs along the chain, either directly in the chain (as for poly(silanes) or PPV) or in the molecules connected to the chain as side groups (as for PVK). In systems in which the charge-transport molecules are present as guests, aggregation of these molecules undoubtedly occurs, which ensures contact between the transport molecules as long as the concentration is above a percolation threshold. However, in single-component polymers the charge-transport

molecules are attached to the chain in random locations with spacings which may be nonoptimal due to dilution by the comonomers, and as a result charge transport may be more difficult. Other disadvantages are the synthetic challenge in making fully functionalized polymers and the lack of flexibility, i.e., new syntheses are needed to modify the polymer.

The first example of a fully functionalized polymer which is a candidate for photorefractivity is a methacrylate polymer containing both carbazole and tricyanovinylcarbazole groups linked to the polymer by an alkylene spacer.[93] Thin films of this polymer (1.4–3.3 μm) were high temperature poled (100 °C, 100 V/μm) and found to have both a high electrooptic coefficient (r_{33} = 6.1 pm/V) and high photoconductivity at 514 nm, near the absorption peak of the charge-transfer band. Gratings were written in these thin films at wavelengths between 550 and 600 nm.[94] Two-beam coupling measurements revealed them to be photochemically induced absorption gratings.

FWM grating measurements were performed on thicker samples (100 μm) in a related[95] acrylate polymer containing the same groups (with a small molecule plasticizer added) at λ = 700 nm with the same geometry described in section II. The sample showed a diffraction efficiency of $\sim 6 \times 10^{-8}$ at a field of 15 V/μm, and $\eta \approx 3 \times 10^{-8}$ with no bias field across the sample. The zero-field effect was attributed to an absorption grating resulting from the periodic space–charge.[95] Although gratings due to diffusion seldom occur in PR polymers, with such a low diffraction efficiency, a weak diffusion grating is possible. No beam-coupling measurements were performed on this material, and therefore no unambiguous proof of the photorefractive origin of the field-dependent gratings in this material exists.

Several other candidate polymers have been reported in the literature. The first[96,97] is poly(vinyl cinnamate) (PVCN)/3-(cinnamoyloxy)-4-[4-(diethylamino)-2-(cinnamoyloxy)phenylazo]nitrobenzene (CNNB-R), a photocross-linkable nonlinear optical polymer. Photoconductivity was reported in this polymer near the absorption peak of the CNNB-R at λ = 514 nm without the addition of a charge-transporting agent. It was suggested that the CNNB-R NLO chromophore was also acting as the charge-transporting agent. No published photorefractive measurements of any type have been reported for this system.

A recent report[98] describes photorefractive measurements on a previously described fully functionalized system[99] in which the NLO chromophore, charge-transporting molecule, and a charge generator were all attached to the same polymer backbone. The NLO chromophore was provided by a monomer with an amino(methylsulfonyl)stilbene functionality, the hole transport was provided by a similar monomer with a diphenylhydrazone similar to DEH, and the charge generator was provided by a third monomer to which one of two different derivatives of Foron brilliant blue was attached. One advantage of this system derives from the fact that in principle the relative concentrations of the various components (and therefore the volume fraction of the three functionalities) can be independently adjusted. The photoconductive response time at 632 nm was observed to be on the order of 100 ms at an intensity of 0.4 W/cm^2, from which a photocurrent quantum yield of 2.6×10^{-3} was reported. However, even though the absorption at this wavelength was appreciable, no values of optical density or absorption coefficient were presented. In a thin film 0.8 μm in thickness, values of r_{33} on the order of 12 pm/V were observed at 632 nm, with only a 5% reduction in this value 3 months after poling.

To test for the presence of PR grating formation, a wave guide geometry was used with poling normal to the wave guide plane.[98] For this geometry, the uniaxial ("3") direction is normal to plane and the grating wave vector lies in the plane, so the usual r_{33} and r_{13} electrooptic coefficients do not apply and the polarization rotation components r_{51} and r_{42} must be utilized (although these facts were not mentioned). Two-beam coupling studies (in an unstated external field) were performed at 632 nm with a 3-mm interaction length, and gain coefficients up to 2.3 cm^{-1} were reported as a function of grating wave vector. Again, without knowledge of the absorption coefficient, the presence or absence of net gain could not be assessed. The authors did not observe a completely asymmetrical energy transfer between the two beams indicating the presence of a photorefractive effect and a photochromic effect (absorption grating). The absorption grating appeared even in an unpoled wave guide and had a measured spatial phase shift of 0 ± 20°. The index grating phase shift was 26 ± 20°, consistent with contributions from a photochromic process and a (phase-shifted) photorefractive process. The relative magnitudes of the gratings from these two processes were not reported. These promising materials should be studied in the future at wavelengths with reduced absorption (or with improved charge generators) in order to try to minimize the photochromic process.

As a final example of a single-component system, a 1:1 side-chain copolymer of (dialkylamino)nitrostilbene on a methacrylate backbone (DANS/MMA) was studied for photorefractivity without the addition of a specific photoconducting component.[100] The photoconductivity at 632 nm was measured to be between 4×10^{-12} and 1×10^{-10} $(\Omega - \text{cm})^{-1}/(\text{W/cm}^2)$, depending upon field. At 632 nm, the absorption was measured to be 3823 cm^{-1}, and in an electrode-poled thin film 8 μm in thickness an electrooptic coefficient of 20 pm/V was observed. Four-wave mixing grating measurements were performed on the 8-μm-thick films with s-polarized writing beams and both s- and p-polarized reading beams using a small grating period of 184 nm. The angle between the grating wave vector and the film plane was not stated, so it is difficult to determine the projection of the wave vector along the poling direction. With a writing intensity of 55 mW/cm^2 per beam and an applied field of 50 V/μm, grating diffraction efficiencies of 10^{-5} were observed with rise and fall times of 1.5–2.5 min and 2–3 min, respectively. The facts that (i) s-wave diffraction was much stronger than p-wave diffraction and (ii) s-wave diffraction was observed even without an applied field led the authors to conclude that the gratings were produced by both photorefractive and nonphotorefractive processes, the latter possibly caused by cis–trans isomerization. Without specific measurements of asymmetric two-beam coupling or grating spatial phase shifts, it is difficult to conclusively determine the origin of the observed gratings.

IV. Theoretical Issues for Photorefractive Polymers

Although little detailed theoretical work has been reported on PR polymers to date, three separate issues have been addressed. The first (section A) concerns the effect of mobility and the quantum efficiency of charge generation on the fundamental limit for the photorefractive response time. This is an important issue because the charge generation efficiency and mobility have substantially lower values in organic polymer systems than in inorganic crystals, and if the response times are to be improved it is necessary to know which physical parameter is limiting the response in the current generation of organic PR polymers. Once this is known, faster systems may be designed.

The second issue (section B) concerns the work that has been done on the solution of the coupled transport and electromagnetic equations which govern the dynamic and steady-state behavior of the PR effect in organic polymers. As discussed in section II.B, the details of the PR effect in polymers are sufficiently different that the standard equations for the PR effect in inorganic crystals[101] need to be modified and solved. Finally, fundamentally new effects may be found in polymeric photorefractive systems, and section C describes the theoretical treatment of one such new effect: an orientational enhancement in the PR diffraction efficiency due to periodic poling of the chromophores by the space-charge field in low T_g polymers in which the chromophores have orientational mobility at ambient temperatures.

A. Role of Mobility and Photocharge Generation Efficiency in Determining Speed

One possible limitation of PR polymers that is often mentioned is the relatively slow speed of response, especially relative to the semiconductor materials. The speed of formation of a space-charge grating is proportional to the photoconductivity which in turn depends upon the quantum yield of photogeneration ϕ, the carrier lifetime, and the mobility of the carriers μ, as described by eq 3. To increase the photoconductivity and hence the speed, it is often assumed that a material with high mobility is required. This section shows by analysis of the photogeneration process that mobility limitations only occur when the photocharge generation process itself is sufficiently efficient.

The temporal response of a PR polymer can be assessed by using a simple model of the maximum sensitivity originally stated by Glass et al.[102,103] and restated by Yeh to estimate the fundamental limit on the speed of the PR effect in inorganic crystals.[104,105] The original development showed that there is a maximum sensitivity of a PR material, where sensitivity is defined as the PR response (usually index change) per unit energy required to produce this response (see section V for precise definitions). Yeh recast this as a limitation on speed given a required beam-coupling gain. For our purposes, the analysis can be further rewritten[43] as an upper limit on the growth rate of the 2BC gain coefficient, given by

$$\left(\frac{\Gamma}{t}\right)_{max} = \left(\frac{h\nu}{c}\right)\left(\frac{\Lambda_G}{\lambda}\right)\left(\frac{\pi}{2}\right)I\left(\frac{n^3 r_e}{\epsilon_0 \epsilon_r}\right)(\alpha\phi) \qquad (10)$$

where all parameters are as previously defined and

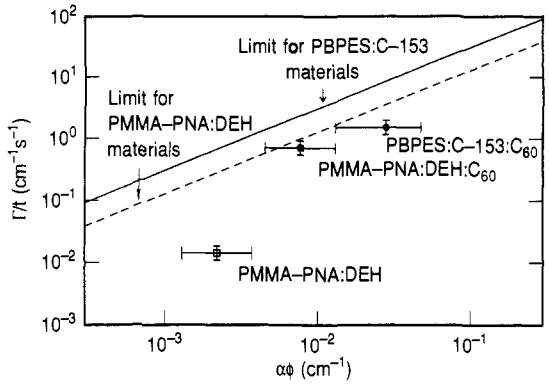

Figure 22. The maximum observed value of Γ/t shown as a function of $\alpha\phi$ for PMMA-PNA:DEH (open square), PMMA-PNA:DEH:C_{60} (filled square), and PBPES:C-153: C_{60} (circle). Also shown are the theoretical limits based on the charge-generation limited model for the PMMA-PNA:DEH materials (dashed line) and PBPES:C-153:C_{60} (solid line). (Reprinted from ref 43. Copyright 1993 Optical Society of America.)

where the rate has been estimated by an equivalent ratio for convenience. This model assumes that the rate-limiting step to the formation of the PR space-charge field at a given wave vector is charge generation; once a charge is generated, the mobility is assumed sufficiently high and the trapping sufficiently efficient that the charge contributes immediately to the PR grating. More precisely, it is assumed that the transport length is optimal, that is, equal to the grating wavelength Λ_G. Any decrease in the rate of grating formation due to inefficient transport and trapping should cause the measured Γ/t to fall below the value predicted by the right-hand side of eq 10.

For the PR polymer PMMA-PNA:DEH, both with and without a sensitizing agent, the previously reported[79] values for all of the parameters in eq 10 are $n^3 r_e$ = 0.5 pm/V at E_0 = 11.4 V/μm, $\epsilon_r \approx 9$, λ = 647 nm, and Λ_G = 1.6 μm. These values fix a linear relation between Γ/t (or an equivalent derivative) and $\alpha\phi$, which is shown on Figure 22 (dashed line). For the actual material (which has no explicit sensitizer), the value observed for Γ/t falls well below the fundamental limit for the measured values of α = 3.7 cm^{-1} and $\phi = 6 \times 10^{-4}$ (open square). For the polymer doped with 0.1 wt % C_{60}, the maximum value of Γ/t increases to a value near the predicted limit for the measured values of α = 6.4 cm^{-1} and $\phi = 1.2 \times 10^{-3}$ (filled square). This is due to both an increase in the value of Γ and a decrease in the response time t. It has been suggested previously that the addition of C_{60} increases the concentration of traps in this PR polymer.[79] Since the addition of 0.2 wt % of C_{60} should have negligible effect on the mobility, it is most likely the improvement in trapping that raises the performance of this material to the generation limit. Without increasing the value of $\phi\alpha$, further increases in the mobility or more efficient charge transport should not improve the gain growth rate by a substantial amount in this polymer.

The poly(silane)-based polymer PBPES:C-153:C_{60} provides an example to illustrate the generation limit for a sample with much higher mobility (and different $\phi\alpha$).[43] In this material, the mobility at high fields reaches 10^{-3} cm^2/(V s), approximately 2–3 orders of magnitude higher than the other PR polymers. Using

the values $n^3r_e = 0.8$ pm/V, (an estimated value for $E_0 = 11.4$ V/μm), $\epsilon_r \approx 6$, $\lambda = 647$ nm, and $\Lambda_G = 1.6$ μm, the generation limit is shown on Figure 22 (solid line). It should be noted that there is a larger uncertainty in the right-hand side of eq 10 for this material than for PMMA-PNA:DEH, due to the difficulty in accurately measuring n^3r_e in the presence of the strong piezoelectric effect. The peak value for Γ/t is shown in Figure 22 (filled circle) for the measured values of $\alpha = 14$ cm^{-1} and $\phi = 2.0 \times 10^{-3}$.

The experimentally determined value of Γ/t falls further below the line for the PBPES:C-153:C_{60} sample than for the PMMA-PNA:DEH:C_{60} sample. A slightly higher value of Γ/t is achieved in the poly(silane)-based material due to a combination of increases in the product $\alpha\phi$, the mobility, and possibly improved trapping. Since $\alpha\phi$ increases by a factor of 3 and μ increases by a factor of 100, the modest size of the increase in Γ/t implies relatively inefficient trapping dynamics compared to PMMA-PNA:DEH:C_{60}.

It seems clear that the PR performance of these materials is not mobility limited. An increase in μ by 2 orders of magnitude over that of PMMA-PNA:DEH:C_{60} has only a small effect on the measured Γ/t. Optimization of the traps should lead to faster performance much closer to the generation limit. Since the total absorption of the material will likely be bounded by thermal and photochemical effects which can occur at large α, the route to even faster organic PR polymers lies in increasing the quantum efficiency of charge generation, either though higher applied fields or intrinsically more efficient sensitizers.

B. Theories for the Space-Charge Field

1. Modifications of Kukhtarev Theory To Include Geminate Recombination

The original rate equation theory of Kukhtarev[101] was intended to describe the generation of a space-charge field due to nonuniform illumination of an inorganic photorefractive material. The approach utilized a standard current equation, a continuity equation (for a single mobile charged species), Poisson's equation to relate the internal field to the charge density, and a rate equation for the single charged species. While this model has formed a very useful solid foundation for the interpretation of the grating experiments on inorganics,[106] it contains several shortcomings when organic materials are considered. One limitation is related to the assumption of a field-independent photocarrier generation quantum yield ϕ. In organic materials, quantum yields of charge generation are known to be highly field dependent[30] due to the tendency of a germinate pair once formed to recombine unless an electric field is present to assist in charge separation.

The first theoretical effort[107] to include field-dependent generation added a limiting form of the Onsager model[29] of charge generation to the basic Kukhtarev theory. In a material (actually a liquid) characterized by a dielectric constant, Onsager calculated the probability that a thermalized electron-hole pair initially separated by a fixed distance (due to the excess energy provided by the optical absorption) will recombine due to the mutual Coulomb attraction. The yield of charge carriers that escape is strongly dependent upon both the temperature and the electric field. Of interest here is the fact that due to screening, the range of the Coulomb attraction increases with lower dielectric constant, thus one would expect that higher fields would be required to overcome geminate recombination in organic materials.

Twarowski[107] used the expansion of the Onsager field-dependent charge generation probability to first order in E to modify the ϕ in the Kukhtarev equations:

$$\phi(E) = \phi_0 \exp(-r_c/r_0)[1 + (E/2E_c)] \qquad (11)$$

where r_0 is the initial separation of the charge carrier and its donor, ϕ_0 is the quantum yield of thermalized carriers (in zero field), $r_c = e^2/4\pi\epsilon_r\epsilon_0 k_B T$ is the Coulomb separation where the Coulomb energy equals the thermal energy, and $E_c = k_B T/er_c$ is a characteristic field. Values[107] of the initial separation parameter r_0 range from 2.5 nm for PVK-TNF to 6.7 nm for crystalline anthracene, and E_c is approximately 1×10^6 V/m for $\epsilon_r = 3$. Due to the linear expansion of the complete Onsager field dependence, the specific results are only valid for $E \ll E_c$; however, at higher fields the quantum yield continues to increase as higher powers of the applied field enter, and at extremely high fields the quantum yield saturates at values near unity.[30]

The modified Kukhtarev equations were solved[107] in the linearized regime under the assumption of small optical intensity modulation $m \ll 1$. The results of the analysis clearly depend upon the ratio of r_c to r_0, which can be as large as 6–9 in some organics. While the saturation values for the internal space-charge field are not greatly affected by geminate recombination, in materials with low dielectric constant at low field where the quantum yield is small, the response times for grating formation and optical erasure would be expected to be long. For example, in zero field, the grating erasure time for choices of parameters suitable for organics would be on the order of 10^5 s at 1 W/cm^2. This is one reason why large fields have been necessary for the observation of true PR gratings in polymeric materials on reasonable time scales.

2. More Complete Rate Equation Models

The early work to include the effects of geminate recombination,[107] although instructive, still did not include (1) the full field dependence of the photogeneration quantum yield,[108] nor (2) the effects of field-dependent mobility, nor (3) the possibility that in a molecularly doped polymer the diffusion coefficient for carriers may not be related to the carrier mobility by the usual Einstein relation,[109] nor (4) the possibility that the recombination and trapping rates may be mobility dependent (Langevin recombination[110]). Several approaches are possible to the challenging problem of formulation of more complete microscopic theories for the space-charge field. At this early stage of understanding of PR polymers, it is preferable to consider only the rate equation approach.

The relevant physical processes of photogeneration, recombination, trapping, and thermal detrapping are treated in a fashion similar to that for the inorganics, with special modifications as required to account for the different charge generation and conduction mechanisms. The photogeneration process active in the illuminated regions may be described by

$$G + h\nu \rightarrow G^- + \text{hole} \quad (12)$$

where G designates a generator molecule. The trapping process can be described by

$$\text{Tr} + \text{hole} \rightarrow \text{Tr}^+ \quad (13)$$

where Tr designates an unoccupied trapping site. Assuming two-body recombination and thermally activated detrapping, the full continuity equation is

$$\frac{\partial p}{\partial t} = -\frac{1}{e}\frac{\partial j}{\partial z} + \frac{s\phi I}{h\nu}N_G - (\gamma_T N_T + \gamma_R N_G^-)p - N_T^+ \nu_0 \exp(-\Delta_T/kT) \quad (14)$$

with p = hole density, N_G = generator density, N_G^- = density of reduced generators, N_T = (unoccupied) trap density, N_T^+ = density of occupied traps, j = current density, γ_T = two-body trapping coefficient, γ_R = two-body recombination coefficient, I = irradiance, T = temperature, s = absorption cross section, e = electron charge, $\phi(E)$ = quantum efficiency, and ν_0, Δ_T = thermal detrapping parameters. The expression for the current density due to drift and diffusion is

$$j = e\mu p(E_0 + E_{sc}) + eD\frac{\partial p}{\partial z} \quad (15)$$

with $\mu(E)$ = mobility and D = diffusion coefficient. Poisson's equation provides the crucial link between the total internal field and the space–charge density

$$\frac{\partial(E_0 + E_{sc})}{\partial z} = \frac{e}{\epsilon_r \epsilon_0}(p + N_T^+ - N_G^-) \quad (16)$$

Rate equations for the traps and the generators are given by

$$\frac{\partial N_G^-}{\partial t} = \frac{s\phi I}{h\nu}N_G - \gamma_R p N_G^- \qquad \frac{\partial N_T^+}{\partial t} = \gamma_T p N_T - N_T^+ \nu_0 \exp(-\Delta_T/kT) \quad (17)$$

The conservation of sites is expressed by

$$N_G^0 = N_G + N_G^- \qquad N_T^0 = N_T + N_T^+ \quad (18)$$

These equations must be solved with the assumed optical intensity pattern

$$I = I_0(1 + m\cos K_G z) \quad (19)$$

where m is the contrast of the interference pattern. Specific models must be assumed for the field dependence of ϕ, μ, and the recombination rate constants in order to complete the physical model. It is clear that this set of equations cannot be solved exactly, so two approaches are available: numerical solution and linearization.

By considering several limiting cases, Schildkraut et al. have illustrated both approaches to the solution of these equations. In the first study,[111] numerical simulation was utilized to calculate the space–charge field produced by photogeneration, transport, and trapping of mobile holes. The photogeneration quantum yield was assumed to follow $\phi(E) = E^p$, where p is unity; this behavior is consistent with the behavior of some organic materials in the field range well below saturation. The field dependence of the mobility was taken as $\mu = \exp[C(E^{1/2} - 1)]$ with C an experimentally determined constant. Examples with this mobility dependence are common in the literature on photoconducting polymers.[34-38] Both recombination and trapping rates were assumed to follow the Langevin form of $\gamma_R = \gamma_T = e\mu/\epsilon_r\epsilon_0$. The Langevin model is appropriate to the case where a mobile carrier and the generation site are both charged so that a strong Coulomb attraction between them controls the recombination probability when they are within a sphere of radius equal to the Coulomb radius r_c. This is a reasonable assumption for the generation process of eq 12 when the generator G is initially uncharged (the usual case). However, Langevin trapping may not be appropriate when the trapping center Tr on the left-hand side of eq 13 is initially neutral.

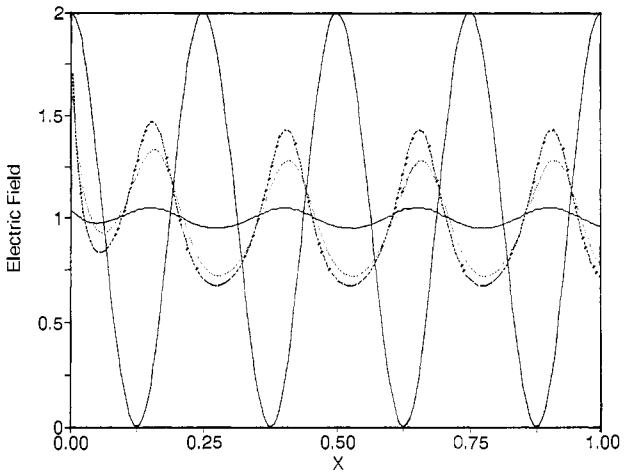

Figure 23. Simulation of internal electric field vs position in normalized units in a dc field of unit value. The heavy solid line shows the light intensity profile for $m = 1$. The electric field is shown by the solid line of small amplitude at reduced time $t = 0.1$ s. The light dashed line at $t = 1.0$ s, and the heavy dashed line at $t = 10.0$ s. (Reprinted from ref 112. Copyright 1992 American Institute of Physics.)

Under these assumptions, numerical simulations were presented[111] for the cases of (1) no traps present and (2) hole trapping with no thermal detrapping. In case 1, a space–charge field is still produced because on average the holes drift away from the generator sites in the large external drift field. In case 2, as expected a larger space–charge field is produced. Figure 23 shows the spatial distribution of the light intensity pattern (heavy solid line of large amplitude) and the calculated amplitude of the space–charge field at reduced times 0.1 (thin solid line), 1.0 (light dashed line), and 10.0 (heavy dashed line). The spatial phase-shift between the light pattern and the peaks of the space–charge field is clearly evident.

In a second study of the rate equation model,[112] analytical solutions were presented for the zero- and first-order Fourier components of the space–charge field. The authors considered two limiting cases: (a) once a charge is trapped, it cannot be released (deep traps) and (b) no hole traps are present. The Einstein relation between the mobility and the diffusion coefficient was assumed in order to remove one unknown physical quantity. The assumption of Langevin trapping described above was relaxed, as the hole traps were not required to be charged. For the deep trap case, a steady-state expression for the first-order Fourier component of the space charge field E_1 was obtained in the limit of high-trap density and small photogeneration relative to trapping. The expression may be

compared to that for the standard PR model[106]

$$E_1 = \frac{mE_q(E_o + iE_d)}{E_q + E_d - iE_o} \tag{20}$$

where $E_q = eN_A(1-N_A/N_D)/(\epsilon_0\epsilon_r K_G)$ is the trap-density-limited space-charge field, N_D is the density of donors, and N_A is the density of acceptors. The corresponding expression for the organic photorefractive material[112] is quite similar, with the density of acceptors replaced by the density of traps, and with additional field-dependent terms arising from the field dependence of mobility and quantum efficiency.

While these calculations provide an important first step toward a model framework for the understanding of PR polymers, these model results must now be tested on actual materials. Moreover, several additional physical effects should be included in future work: (i) the presence of shallow traps as well as deep traps (the evidence for which is the sublinear intensity dependences[75] of the growth rate described for numerous systems in Section III), (ii) a more complete field-dependence of the photogeneration efficiency especially when sensitizers like C_{60} are used,[113] and (iii) trapping mechanisms which do not follow the Langevin form.

C. Orientational Enhancement of the Photorefractive Effect

In the standard model of the PR effect the modulation in the index of refraction due to the internal space-charge field is given by the electrooptic effect as shown in eq 2. Since the electrooptic coefficient is generally assumed to be a constant in this model, it is useful to call this the "simple EO" model for the PR effect. Recently, a new mechanism for a significant enhancement to the simple EO case has been reported in polymers[45] in which the NLO chromophores are small-molecule guests in the polymer matrix. The model system for this effect was PVK:FDEANST:TNF. The enhancement relies on the ability of the NLO chromophores to be aligned not only by the externally applied electric field, but also in situ by the sinusoidally varying space-charge field during grating formation. The resulting spatially periodic poling of the sample leads to a modulation of the birefringence of the material and to a modulation of the electrooptic response, the combination of which contributes favorably to the diffracted fields in the proper polarization.

Figure 24 illustrates the effect schematically. The interfering light beams are assumed to produce a sinusoidally varying space-charge field by the usual mechanisms of drift and diffusion. The externally applied electric field E_0 will add to this field to produce a total field E_T. Since the NLO chromophores have orientational mobility due to the low T_g or to their molecular size, a spatially periodic orientational pattern is produced as the electric field orients the molecules by virtue of their ground-state dipole moment. In the two center panels, the figure illustrates this effect using a locally averaged value of the molecular dipole moment. The two writing beams are assumed to enter the sample from the right and left sides of the figure. If E_{sc} and E_0 lie in the same direction, as in Figure 24, only the magnitude of the average local dipole moment will be periodic. In the more general case, where there is a

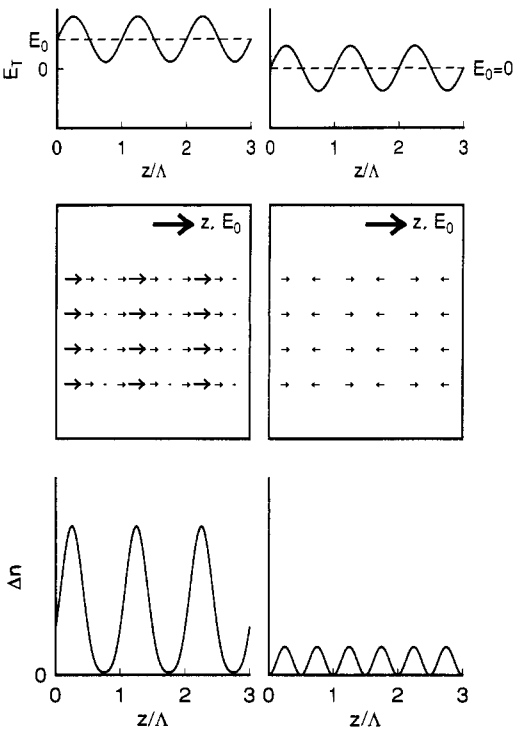

Figure 24. Schematic illustration of the periodic poling responsible for the orientational enhancement effect. For simplicity, the background field E_0 and the space-charge field are both directed along z in this figure, which would occur if the writing beams entered the sample from either side (symmetrically). The magnitude of the total field is shown at the top, for $E_0 \neq 0$ (left) and $E_0 = 0$ (right). The resulting average alignment of the chromophores is shown in the center, and the resulting refractive index grating is shown in the bottom panels. Note that for $E_0 = 0$, there is no component of the Δn grating at $1K_G$, while for $E_0 \neq 0$ a modulation at $1K_G$ appears. When the grating is written in the oblique geometry shown in Figure 4, there is a (uniform) component of the dc electric field perpendicular to z as well, resulting in a modulated direction as well as magnitude of the periodic poling field.

component of E_0 orthogonal to E_{sc}, the direction of the average local dipole moment will be periodic as well. Reference 45 treats the general case of oblique incidence (Figure 4) in detail.

The effect of the periodic orientation is to produce a modulated birefringence and a modulated EO coefficient, both of which can contribute to the scattered light field. For these two effects, the nonlinear response of the material is quadratic in the total local electric field; hence the orientational enhancement effect may be regarded formally as a $\chi^{(3)}$ process. However, this orientational $\chi^{(3)}$ arises from different physical processes than other $\chi^{(3)}$ mechanisms previously reported for a variety of semiconductor and quantum well systems[64-66] based on Franz-Keldysh and band-edge effects and from the quadratic response in paraelectric crystals like potassium tantalate niobate.[67,68] As Figure 24 illustrates (right side), if no dc electric bias field is present, the resulting modulation of the index of refraction is at twice the wave vector K_G of the intensity pattern. When a bias field is present (left side of Figure 24), the modulation appears at K_G as well and can contribute strongly to the first-order Bragg-diffracted beam. The orientational enhancement effect should be operative for any photorefractive polymer in which the nonlinear chromophores have the ability to reorient appreciably

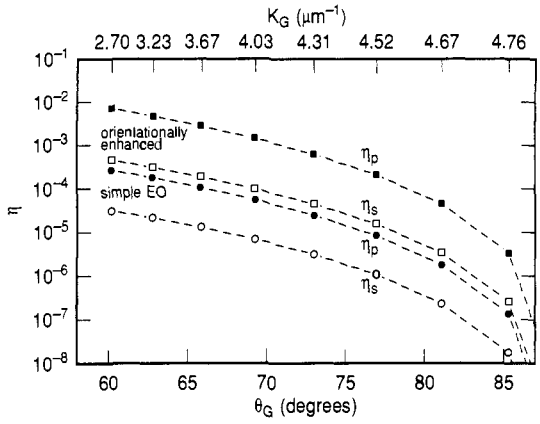

Figure 25. Illustration of the enhancement of the PR diffraction efficiency induced by dynamic orientation. The diffraction efficiencies η_s and η_p predicted by the "simple" EO theory (circles) and the diffraction efficiencies η_s and η_p predicted by the orientational enhancement theory (squares) are shown as a function of θ_G (bottom axis) and K_G (top axis). The space–charge field amplitude E_{sc} is assumed to reach its maximum value $E_{sc} = E_0 \cos\theta_G$; $\lambda = 676$ nm, $d = 125$ μm, and the values of n^3r_{33}, $n^3r_{13} = (1/3)n^3r_{33}$, and other parameters are those found experimentally for PVK:FDEANST:TNF. (Reprinted from ref 45. Copyright 1993 Optical Society of America.)

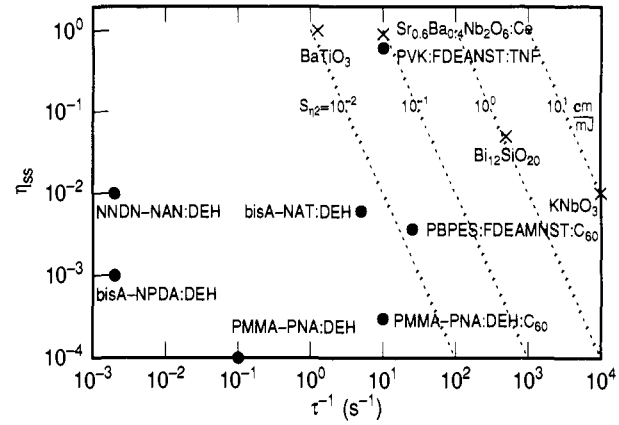

Figure 26. Comparison of several inorganic PR materials and a selection of PR polymers. Saturation diffraction efficiency η_{ss} vs growth rate τ^{-1}, scaling to 1-mm thickness and assuming 1 W/cm^2 writing intensity. The lines are contours of constant sensitivity $S_{\eta 2}$.

in response to the local electric field; in contrast, it should not be important for permanently poled PR polymeric systems nor for PR crystals, either inorganic or organic.

The development of the orientational enhancement mechanism was motivated by the observation that, for the measured diffraction efficiency and electrooptic coefficient, the calculated space–charge field amplitude greatly exceeded the external applied field in PVK:FDEANST:TNF, a situation which cannot occur. The full theory[45] leads to three predictions: (1) an enhanced diffraction efficiency, (2) a change in the polarization anisotropy, and (3) presence of gratings with wave vectors of $2K_G$, $3K_G$, etc., even with a purely sinusoidal space–charge field. The enhancement of the diffraction efficiencies η_s and η_p is illustrated in Figure 25 for a hypothetical material in which the space–charge field amplitude E_{sc} has reached the maximum allowed value, $E_0 \cos\theta_G$. Specific values of the parameters that enter into the calculation are those measured for PVK:FDEANST:TNF.[45] Figure 25 shows the results for a range of grating tilt angles (or grating wave vectors). The open symbols show the values of η_s and the closed symbols the values of η_p. The circles give the expected diffraction efficiencies for the simple EO PR effect, and the squares the diffraction efficiencies including the orientational enhancement. At essentially all angles, the size of the enhancement is approximately a factor of 10 for η_s and more than a factor of about 30 for η_p. This increases the theoretically predicted diffraction efficiency to approximately the levels found experimentally if it is assumed that the space–charge field approaches the value of the external field projected along the grating wave vector. The results of predictions 2 and 3 are also verified for PVK:FDEANST:TNF.[45]

Since the orientational enhancement effect depends upon the ability of the NLO chromophores to dynamically orient during grating formation, the speed of the effect should be limited by the rotational mobility of the chromophores in the PR polymer.[91] These molecular orientation times can range from picoseconds (observed in liquids[114]) to extremely long times of years or more observed in permanently poled polymers,[115] depending upon the viscosity of the material, the size of the chromophore,[92] the presence of plasticizing agents, and other factors. The rotational orientation time should be varied over a large range in future materials to determine the actual limitations on speed of the orientational enhancement effect.

The modulation of poling produces a contribution to the diffraction efficiency even if the modulation of r is ignored and only the modulation of birefringence is present. Hence, chromophores with zero hyperpolarizability but large ground-state dipole moment and large birefringence are potentially useful in the formulation of PR polymers, if such chromophores exist. In addition, if the spatially modulated orientation were frozen in by cooling of the sample before the decay of the space–charge field, the eventual decay of the space–charge field would not cause the diffracted signal from the stored orientation to disappear. This fixing phenomenon could allow nondestructive readout, where the long-term storage of information occurs via storage of a sinusoidal poling of the chromophores.

V. Comparison to Inorganic Crystals and Future Prospects

A. Diffraction Efficiency and Growth Rate

The performance of the recently discovered PR polymers is comparable to that for some of the well-known inorganic photorefractive materials,[2-9] such as $LiNbO_3$, $Bi_{12}SiO_{20}$ (BSO), $KNbO_3$, and $BaTiO_3$. The different materials can be compared using several measures. A direct comparison of two of the most relevant photorefractive properties, steady-state grating diffraction efficiency η_{ss} and growth rate τ^{-1}, is shown in Figure 26, where η_{ss} is plotted as a function of τ^{-1} on a log–log scale. The η_{ss} values are for 1-mm-thick samples, which are measured directly for the inorganic crystals and extrapolated for the organic systems (assuming $\eta \approx d^2$), and the growth rates are for write intensities of 1 W/cm^2. With the exception of PVK:FDEANST:TNF, all of the polymeric photorefractive systems lie in the lower left of Figure 26. This includes the cross-linked epoxy systems bisA-NPDA:DEH[17] and

Table 4. Photorefractive Sensitivities[a]

material	E_0 (V/μm)	$(S_{n_1})^{-1}$ (kJ/cm³)	$(S_{n_2})^{-1}$ (kJ/cm²)	$(S_{\eta_1})^{-1}$ (mJ/cm²)	$(S_{\eta_2})^{-1}$ (mJ/cm)
bisA-NPDA:DEH	11.4	7×10^4	7×10^3	1×10^6	2×10^5
PMMA-PNA:DEH:C_{60}	11.4	1 500	150	25 000	2 500
bisA-NAT:DEH	56	1 000	25	17 000	430
PBPES:FDEAMNST:C_{60}	11.4	170	25	2 900	420
PVK:FDEANST:TNF	40	100	5.9	1 700	100
$LiNbO_3$	(PV)	20–200		1 000	300
	5 (PC)		6		
$BaTiO_3$	(PV)			50–1 000	
	1 (PC)			0.1–10	
SBN	(PV)	12–75	7.2–30	2.5–15	1.6–6
BSO	0.6 (PC)	0.014	0.006	0.7	0.3
$KNbO_3$	(PV)	6–60	0.1		
	0.7 (PC)	0.08	0.02		

[a] Inorganic crystal values from ref 116.

NNDN-NAN:DEH,[61] PMMA-PNA:DEH, both unsensitized[72] and sensitized with C_{60},[79] and bisA-NAT:DEH.[80] PVK:FDEANST:TNF lies near the upper right of Figure 26, along with the inorganic photorefractive materials. The large diffraction efficiency and net gain observed in PVK:FDEANST:TNF, along with the material advantages which accompany a polymeric system should heighten the interest in practical device applications for PR polymers.

B. Photorefractive Sensitivities

Another method of comparing the performance of various photorefractive materials is through their photorefractive sensitivities. Four different photorefractive sensitivities have been used in the literature[5]

$$S_{n1} = (1/\alpha)(\partial n_i/\partial W_0) \quad (21)$$

$$S_{n2} = \partial n_i/\partial W_0 \quad (22)$$

$$S_{\eta 1} = (1/\alpha d)(\partial \eta^{1/2}/\partial W_0) \quad (23)$$

$$S_{\eta 2} = (1/d)(\partial \eta^{1/2}/\partial W_0) \quad (24)$$

where W_0 is the incident fluence or optical energy per unit area. The first two sensitivities, S_{n1} and S_{n2}, are the refractive index change per unit absorbed energy and volume and the refractive index change per unit incident fluence, respectively. $S_{\eta 1}$ and $S_{\eta 2}$ are the changes in the square root of the diffraction efficiency per unit absorbed energy and volume and unit incident fluence, both for unit crystal length. These latter two sensitivities are more directly determined from experimental measurements of η. All sensitivities are defined at the initial stage of hologram formation. These sensitivities are also valid for holographic gratings formed by mechanisms other than photorefractivity.

A comparison of these sensitivities for various PR polymers as well as some inorganic crystals[116] are shown in Table 4. As is customary in the inorganic literature, the inverse of the sensitivities have been tabulated, along with the applied field E_0 for the polymeric materials and the inorganic crystals in the photoconductive (PC) mode of operation (PV = photovoltaic mode; no applied field). Smaller values of the inverse sensitivity represent better performance. The photorefractive sensitivity of PVK:FDEANST:TNF ($(S_{n1})^{-1}$ = 100 kJ/cm³) is observed to be comparable to that of $LiNbO_3$, SBN, and $KNbO_3$ in the photovoltaic mode, which is expected from the comparison shown in Figure 26. Other inorganic materials have significantly higher sensitivities, such as $KNbO_3$ (PC) and BSO, which have sensitivities near the theoretical limit[116] $(S_{n1})^{-1} = 0.002$ kJ/cm³ for the PR effect. However, the high sensitivities of BSO and $KNbO_3$ are also accompanied by lower ultimate diffraction efficiencies (see Figure 26). Lines of constant sensitivity ($S_{\eta 2}$) are also shown in Figure 26, for values of $S_{\eta 2} = 10^{-2}$, 10^{-1}, 10^0, and 10^1 cm/mJ.

C. Outlook

Consideration of some of the limitations of the current PR polymers provides a guide to issues which should be addressed in future research efforts. The problems may be divided roughly into two areas: fabrication-related issues and mechanistic issues. On the fabrication side, in order to achieve larger diffraction efficiencies and useful beam-coupling gain, methods must be devised for making thicker samples while not sacrificing the poling-induced nonlinearity. Samples with multiple layers forming a stratified volume holographic optical element[117] should be fabricated to achieve this. Wave-guide geometries provide special difficulties since the poling direction should have a component along the space-charge field, but since thin films are easy to fabricate from PR polymers, this area merits investigation. Other geometries, such as a rodlike geometry which has provided advantages for strontium barium niobate crystals,[118] should be easy to achieve with PR polymers and should be considered.

On the mechanistic side, the sensitivity, or PR response per unit time, must be improved further by a combination of enhancements in both optical nonlinearity and transport, and this area has been discussed in some detail in sections IV.A and IV.C. Little is known about the exact nature of the traps, and the depth and density of the trapping states should be optimized to provide long dark lifetimes for storage applications. Since holograms are usually partially erased during the reading process, fixing mechanisms and two-color writing mechanisms[119,120] should be investigated. The issue of fatigue in a large number of read–write cycles is important for applications and must be addressed. Finally, the structure–property relationships for PR polymers are only partially established, so mechanistic and modeling efforts should continue in order to provide

improved understanding of the ultimate limits of performance and eventually predictive ability for the formulation of PR polymers.

In spite of the numerous areas for future work, the progress in the area of PR polymers so far has been quite rapid, and the most recent materials have already reached the performance levels of some of the well-known inorganic photorefractive crystals in diffraction efficiency, speed, sensitivity, and beam-coupling gain. The very fact that a large number of new materials has appeared in a short time period is a testament to the flexibility of polymers in accepting multiple dopants in large concentration. It is clear that the ultimate limits of these materials have not yet been reached, and further multidisciplinary efforts to devise new PR polymers should continue in order to take advantage of the low dielectric constant, low cost, and flexibility of this new and emerging class of advanced materials.

Acknowledgments. We wish to acknowledge the Advanced Research Projects Agency, Defense Sciences Office, contract no. DAAB07-91-C-K767 for partial support of this work, and we thank G. C. Bjorklund, D. M. Burland, R. D. Miller, J. C. Scott, R. J. Twieg, C. A. Walsh, and C. G. Willson for stimulating discussions and support throughout this work.

References

(1) Chen, F. S. *J. Appl. Phys.* **1967**, *38*, 3418.
(2) Günter, P. *Phys. Rep.* **1982**, *93*, 199.
(3) Feinberg, J. In *Optical Phase Conjugation*; Fisher, R. A., Ed.; Academic Press: New York, 1983; pp 417–443.
(4) Hall, T. J.; Jaura, R.; Connors, L. M.; Foote, P. D. *Prog. Quant. Electr.* **1985**, *10*, 77.
(5) Günter, P., Huignard, J.-P., Eds. *Photorefractive Materials and Their Applications I & II*; Springer Verlag: Berlin; 1988.
(6) Valley, G. C.; Klein, M. B.; Mullen, R. A.; Rytz, D.; Wechsler, B. *Ann. Rev. Mater. Sci.* **1988**, *18*, 165.
(7) Feinberg, J. *Phys. Today* **1988**, *41*, 46.
(8) Petrov, M. P.; Stepanov, S. I.; Khomenko, A. V. *Photorefractive Crystals in Coherent Optical Systems*; Springer-Verlag: Berlin; 1991.
(9) Yeh, P. *Introduction to Photorefractive Nonlinear Optics*; John Wiley: New York, 1993.
(10) Eichler, H. J.; Günter, P.; Pohl, D. W. *Laser-Induced Dynamic Gratings*; Springer Series in Optical Sciences, Vol. 50; Springer: Berlin, 1986.
(11) See, for examples: Brown, G. H., Ed. *Photochromism*; Techniques of Chemistry, Vols. I-III; Wiley-Interscience: New York; 1971.
(12) Valley, G. C. *J. Opt. Soc. Am. B* **1984**, *1*, 868.
(13) Chemla, D. S., Zyss, J., Eds. *Nonlinear Optical Properties of Organic Molecules and Crystals*; Academic Press: Orlando, 1987; Vols. 1 and 2.
(14) Ducharme, S.; Scott, J. C.; Twieg, R. J.; Moerner, W. E. Postdeadline Paper, OSA Annual Meeting, 1990, Boston, MA, November 5–9.
(15) Sutter, K.; Hullinger, J.; Günter, P. *Solid State Commun.* **1990**, *74*, 867.
(16) Sutter, K.; Günter, P. *J. Opt. Soc. Am. B* **1990**, *7*, 2274.
(17) Ducharme, S.; Scott, J. C.; Twieg, R. J.; Moerner, W. E. *Phys. Rev. Lett.* **1991**, *66*, 1846.
(18) Eich, M.; Reck, B.; Yoon, D. Y.; Willson, C. G.; Bjorklund, G. C. *J. Appl. Phys.* **1989**, *66*, 3241.
(19) Schildkraut, J. S. *Appl. Phys. Lett.* **1991**, *58*, 340.
(20) Donckers, M. C. J. M.; Silence, S. M.; Walsh, C. A.; Hache, F.; Burland, D. M.; Moerner, W. E.; Twieg, R. J. *Opt. Lett.* **1993**, *18*, 1044.
(21) Kogelnik, H. *Bell Syst. Tech. J.* **1969**, *48*, 2909.
(22) Cronin-Golomb, M.; Yariv, A. *J. Appl. Phys.* **1985**, *57*, 4906.
(23) Anderson, D. Z.; Lininger, D. M.; Feinberg, J. *Opt. Lett.* **1987**, *12*, 123.
(24) Anderson, D. Z.; Feinberg, J. *IEEE J. Quant. Elec.* **1989**, *25*, 635.
(25) Feinberg, J. *Opt. Lett.* **1982**, *7*, 486.
(26) Feinberg, J. In *Optical Phase Conjugation*; Fisher, R. A., Ed.; Academic Press: New York, 1983; pp 417–443.
(27) Huignard, J. P.; Marrakchi, A. *Opt. Commun.* **1981**, *38*, 249.
(28) Bylsma, R. B.; Olson, D. H.; Glass, A. M. *Opt. Lett.* **1988**, *13*, 853.
(29) Onsager, L. *Phys. Rev.* **1938**, *54*, 554.
(30) Melz, P. J. *J. Chem. Phys.* **1972**, *57*, 1694.
(31) Chance, R. R.; Braun, C. L. *J. Chem. Phys.* **1976**, *64*, 3573.
(32) Braun, C. L. *J. Chem. Phys.* **1984**, *80*, 4157.
(33) Stolka, M. In *Encyclopedia of Polymer Science and Engineering*; John Wiley: New York, 1988; Vol. 11, pp 154–175.
(34) Mack, J. X.; Schein, L. B.; Peled, A. *Phys. Rev. B* **1989**, *39*, 7500.
(35) Schein, L. B. *Philos. Mag. B* **1992**, *65*, 795.
(36) Abkowitz, M. A. *Philos. Mag. B* **1992**, *65*, 817.
(37) Borsenberger, P. M. *Phys. Stat. Sol. B* **1992**, *173*, 671.
(38) Bässler, H. *Phys. Stat. Sol. B* **1993**, *175*, 15.
(39) Scott, J. C.; Pautmeier, L. Th.; Moerner, W. E. *J. Opt. Soc. Am. B* **1992**, *9*, 2059.
(40) Scott, J. C.; Pautmeier, L. Th.; Moerner, W. E. *Synth. Methods* **1992**, *54*, 9.
(41) Scott, J. C.; Pautmeier, L. Th.; Moerner, W. E.; Walsh, C. A.; Silence, S. M.; Matray, T. J.; Twieg, R. J. *Proc. Mat. Res. Soc.* **1992**, *277*, 135.
(42) Stolka, M.; Abkowitz, M. A. *Mat. Res. Soc. Symp. Proc.* **1992**, *277*, 15.
(43) Silence, S. M.; Scott, J. C.; Hache, F.; Ginsburg, E. J.; Jenkner, P. K.; Miller, R. D.; Twieg, R. J.; Moerner, W. E. *J. Opt. Soc. Am. B* **1993**, *10*, in press.
(44) For a recent review, see: Burland, D. M.; Walsh, C. A.; Twieg, R. J. *Chem. Rev.* **1994**, *94*, this issue.
(45) Moerner, W. E.; Silence, S. M.; Hache, F.; Bjorklund, G. C. *J. Opt. Soc. Am. B* **1994**, *11*, in press.
(46) See: Klein, M. B. In *Photorefractive Materials and Their Applications I*; Günter, P., Huignard, J.-P., Eds.; Springer Verlag: Berlin, 1988; Chapter 7, pp 195–236.
(47) Valley, G. C.; Klein, M. B. *Opt. Eng.* **1983**, *22*, 704.
(48) Kavarnos, G. J.; Turro, N. J. *Chem. Rev.* **1986**, *86*, 401.
(49) Dolezalek, F. K. In *Photoconductivity and Related Phenomena*; Mort, J., Pai, D. M., Eds.; Elsevier: Amsterdam, 1976; p 27.
(50) Scott, J. C.; Pautmeier, L. Th.; Schein, L. *Phys. Rev. B* **1992**, *46*, 8603.
(51) Siegelle, M.; Hierle, R. *J. Appl. Phys.* **1981**, *52*, 4199.
(52) Singer, K. D.; Kuzyk, M. G.; Holland, W. R.; Sohn, J. E.; Lalama, S. J.; Comizzoli, R. B.; Katz, H. E.; Schilling, M. L. *Appl. Phys. Lett.* **1988**, *53*, 1800.
(53) Schildkraut, J. S. *Appl. Opt.* **1990**, *29*, 2839.
(54) Teng, G. C.; Man, H. T. *Appl. Phys. Lett.* **1990**, *56*, 1734.
(55) Horsthuis, W. H. G.; Krijnen, G. J. M. *Appl. Phys. Lett.* **1990**, *55*, 616.
(56) Valley, J. F.; Wu, J. W.; Valencia, C. L. *Appl. Phys. Lett.* **1990**, *57*, 1084.
(57) Smith, B. A.; Jurich, M.; Moerner, W. E.; Fleming, W.; Swalen, J. D.; Bjorklund, G. C.; Volksen, W. to appear in *Proc. Soc. Photo-Opt Instrum. Eng.* **1994**, *2025*.
(58) Nye, J. F. *Physical Properties of Crystals*; Oxford: London, 1957.
(59) Ducharme, S.; Feinberg, J.; Neurgaonkar, R. *IEEE J. Quant. Electron.* **1987**, *23*, 2116.
(60) Kuzyk, M. G.; Sohn, J. E.; Dirk, C. W. *J. Opt. Soc. Am. B* **1990**, *7*, 842.
(61) Moerner, W. E.; Walsh, C.; Scott, J. C.; Ducharme, S.; Burland, D. M.; Bjorklund, G. C.; Twieg, R. J. *Proc. Soc. Photo-Opt. Instrum. Eng.* **1991**, *1560*, 278.
(62) Williams, D. J. In *Nonlinear Optical Properties of Organic Molecules and Crystals*; Chemla, D. S., Zyss, J., Eds.; Academic Press: Orlando, 1987; Chapter II-7.
(63) Walsh, C. A.; Moerner, W. E. *J. Opt. Soc. Am. B* **1992**, *9*, 1642; **1993**, *10*, 753.
(64) Partovi, A.; Kost, A.; Garmire, E. M.; Valley, G. C.; Klein, M. B. *Appl. Phys. Lett.* **1990**, *56*, 1089.
(65) Nolte, D. D.; Olson, D. H.; Doran, G. E.; Knox, W. H.; Glass, A. M. *J. Opt. Soc. Am. B* **1990**, *7*, 2217.
(66) Millerd, J. E.; Koehler, S. D.; Garmire, E. M.; Partovi, A.; Glass, A. M.; Klein, M. B. *Appl. Phys. Lett.* **1990**, *57*, 2776.
(67) Agranat, A.; Yacoby, Y. *J. Opt. Soc. Am. B* **1988**, *5*, 1792.
(68) Agranat, A.; Leyva, V.; Yariv, A. *Opt. Lett.* **1989**, *14*, 1017.
(69) Schein, L. B. *Electrophotography and Development Physics*; Springer: Berlin, 1988.
(70) Sturmer, D. M.; Heseltine, D. W. In *The Theory of the Photographic Process*, 4th ed.; James, T. H., Ed.; Macmillan: New York, 1977; pp 194–234.
(71) Schein, L. B.; Rosenberg, A.; Rice, S. L. *J. Appl. Phys.* **1986**, *60*, 4287.
(72) Silence, S. M.; Walsh, C. A.; Scott, J. C.; Matray, T. J.; Twieg, R. J.; Hache, F.; Bjorklund, G. C.; Moerner, W. E. *Opt. Lett.* **1992**, *17*, 1107.
(73) Bashaw, M. C.; Ma, T.-P.; Barker, R. C.; Mroczkowski, S.; Dube, R. R. *Phys. Rev. B* **1990**, *42*, 5641.
(74) Ducharme, S.; Feinberg, J. *J. Appl. Phys.* **1984**, *56*, 839.
(75) Mahgerefteh, D.; Feinberg, J. *Phys. Rev. Lett.* **1990**, *64*, 2195.
(76) Tayebati, P.; Feinberg, J. *J. Opt. Soc. Am. B* **1992**, *8*, 1053.
(77) Cui, Y.; Zhang, Y.; Prasad, P. N.; Schildkraut, J. S.; Williams, D. J. *Appl. Phys. Lett.* **1992**, *61*, 2132.
(78) Robello, D. R.; Dao, P. T.; Phelan, J.; Revelli, J.; Schildkraut, J. S.; Scozzafava, M.; Ulman, A.; Willand, C. S. *Chem. Mater.* **1992**, *4*, 425.
(79) Silence, S. M.; Walsh, C. A.; Scott, J. C.; Moerner, W. E. *Appl. Phys. Lett.* **1992**, *61*, 2967.

(80) Silence, S. M.; Hache, F.; Donckers, M.; Walsh, C. A.; Burland, D. M.; Bjorklund, G. C.; Twieg, R. J.; Moerner, W. E. *Proc. Soc. Photo-Opt. Instrum. Eng.* **1993**, *1852*, 253.
(81) Jungbauer, D.; Teraoka, I.; Yoon, D. Y.; Reck, B.; Swalen, J. D.; Twieg, R.; Willson, C. G. *J. Appl. Phys.* **1991**, *69*, 8011.
(82) Twieg, R. J.; Ebert, M.; Jungbauer, D.; Lux, M.; Reck, B.; Swalen, J. D.; Teraoka, I.; Willson, C. G.; Yoon, D. Y.; Zentel, R. *Mol. Cryst. Liq. Cryst.* **1992**, *217*, 19.
(83) Ducharme, S.; Jones, B.; Takacs, J. M.; Zhang, L. *Opt. Lett.* **1993**, *18*, 152.
(84) Obrzut, J.; Obrzut, M. J.; Karasz, F. E. *Synth. Met.* **1989**, *29*, E103.
(85) Gelsen, O. M.; Bradley, D. D. C.; Murata, H.; Tsutsui, T.; Saito, S.; Rühe, J.; Wegner, G. *Synth. Met.* **1991**, *41*, 875.
(86) Zhang, Y.; Cui, Y.; Prasad, P. N. *Phys. Rev. B* **1992**, *46*, 9900.
(87) Obryzuk, M. E.; Zieba, J.; Prasad, P. N. In *Conference on Lasers and Electro-Optics 1993*, OSA Technical Digest Series; Optical Society of America: Washington, DC, 1993; Vol. 11 p 518.
(88) Pope, M.; Swenberg, C. E. *Electronic Processes in Organic Crystals*; Clarendon: Oxford, 1982; p 748.
(89) Silence, S. M.; Donckers, M. C. J. M.; Walsh, C. A.; Burland, D. M.; Twieg, R. J.; Moerner, W. E. *Appl. Opt.* **1993**, in press.
(90) See, for example: Cheng, L. T.; Tam, W.; Marder, S. R.; Stiegman, A. E.; Rikken, G.; Spangler, C. W. *J. Phys. Chem.* **1991**, *95*, 10643.
(91) Boyd, G. T.; Francis, C. V.; Trend, J. E.; Ender, D. A. *J. Opt. Soc. Am. B* **1991**, *8*, 887.
(92) Hampsch, H. L.; Yang, J.; Wong, G. K.; Torkelson, J. M. *Polym. Commun.* **1989**, *30*, 40.
(93) Tamura, K.; Padias, A. B.; Hall, H. K., Jr.; Peyghambarian, N. *Appl. Phys. Lett.* **1992**, *60*, 1803.
(94) Peyghambarian, N.; Tamura, K.; Kippelen, B.; Kawabe, Y.; Jarka, F.; Mazumdar, S.; Guo, D. D.; Hall, H. K., Jr.; Padias, A. B. *Mat. Res. Soc. Sym. Proc.* **1992**, *277*, 145.
(95) Kippelen, B.; Tamura, K.; Peyghambarian, N.; Padias, A. B.; Hall, H. K., Jr. *J. Appl. Phys.* **1993**, *74*, 3617.
(96) Li, J.; Lee, J. Y.; Yang, Y.; Kumar, J.; Tripathy, S. K. *Appl. Phys.* **1991**, *B53*, 279.
(97) Li, J.; Jeng, R. J.; Kamath, M.; Kumar, J.; Tripathy, S. K. *Mat. Res. Soc. Sym. Proc.* **1992**, *277*, 160.
(98) Yu, L.; Chan, W.; Bao, Z.; Cao, S. X. F. *Macromolecules* **1993**, *26*, 2216.
(99) Yu, L.; Chan, W.; Bao, Z.; Cao, S. X. F. *Polym. Prepr.* **1992**, *33*, 398.
(100) Sansome, M. J.; Teng, C. C.; East, A. J.; Kwiatek, M. S. *Opt. Lett.* **1993**, *18*, 1400.
(101) Kukhtarev, N. V.; Markov, V. B.; Soskin, M.; Vinetskii, V. L. *Ferroelectrics* **1979**, *22*, 949; 961.
(102) von der Linde, D.; Glass, A. M. *Appl. Phys.* **1975**, *8*, 85.
(103) Glass, A. M. *Opt. Eng.* **1978**, *17*, 470.
(104) Yeh, P. *Appl. Opt.* **1987**, *26*, 602.
(105) Glass, A. M.; Klein, M. B.; Valley, G. C. *Appl. Opt.* **1987**, *26*, 3189.
(106) Valley, G. C.; Lam, J. F. In *Photorefractive Materials and Their Applications I*; Günter, P., Huignard, J.-P., Eds.; Springer Verlag: Berlin, 1988; pp 75–98.
(107) Twarowski, A. *J. Appl. Phys.* **1989**, *65*, 2833.
(108) Mozumder, A. *J. Chem. Phys.* **1974**, *60*, 4300, 4305.
(109) Pautmeier, L.; Richert, R.; Bässler, H. *Philos. Mag. B* **1991**, *63*, 587.
(110) Helfrich, W. In *Physics and Chemistry of the Organic Solid State III*; Fox, D., Labes, M. M., Weissberger, A., Eds.; Wiley-Interscience: New York, 1967; pp 22–25.
(111) Schildkraut, J. S.; Buettner, A. V. *J. Appl. Phys.* **1992**, *72*, 1888.
(112) Schildkraut, J. S.; Cui, Y. *J. Appl. Phys.* **1992**, *72*, 5055.
(113) Wang, Y. *Nature* **1992**, *356*, 585.
(114) Berne, B. J.; Pecora, R. *Dynamic Light Scattering*; Wiley: New York, 1976; pp 144–151.
(115) Stähelin, M.; Burland, D. M.; Ebert, M.; Miller, R. D.; Smith, B. A.; Twieg, R. J.; Volksen, W.; Walsh, C. A. *Appl. Phys. Lett.* **1992**, *61*, 1626.
(116) Günter, P.; Huignard, J.-P. In *Photorefractive Materials and Their Applications I*; Günter, P., Huignard, J.-P., Eds.; Springer Verlag: Berlin, 1988; Chapter 2, pp 7–73.
(117) Johnson, R. V.; Tanguay, A. R., Jr. *Opt. Lett.* **1988**, *13*, 189.
(118) Hesselink, L.; Redfield, S. *Opt. Lett.* **1988**, *13*, 877.
(119) von der Linde, D.; Glass, A. M.; Rodgers, K. F. *J. Appl. Phys.* **1976**, *147*, 217.
(120) Bjorklund, G. C.; Bräuchle, Chr.; Burland, D. M.; Alvarez, D. C. *Opt. Lett.* **1981**, *6*, 159.